

# **Numerical Investigation of the Behaviour of High Strength Steel Extended End-Plate Connections**

**Nariman Afzali**

Submitted to the  
Institute of Graduate Studies and Research  
in partial fulfillment of the requirements for the Degree of

Master of Science  
in  
Civil Engineering

Eastern Mediterranean University  
July 2012  
Gazimağusa, North Cyprus

Approval of the Institute of Graduate Studies and Research

---

Prof. Dr. Elvan Yılmaz  
Director

I certify that this thesis satisfies the requirements as a thesis for the degree of Master of Science in Civil Engineering.

---

Asst. Prof. Dr. Murude Çelikağ  
Chair, Department of Civil Engineering

We certify that we have read this thesis and that in our opinion it is fully adequate in scope and quality as a thesis for the degree of Master of Science in Civil Engineering.

---

Asst. Prof. Dr. Murude Çelikağ  
Supervisor

---

Examining Committee

1. Asst. Prof. Dr. Giray Ozay
2. Asst. Prof. Dr. Erdinç Soyer
3. Asst. Prof. Dr. Murude Çelikağ

---

---

---

## ABSTRACT

Using high strength steel has some advantage like reducing weight of the structures. That means less consumption of steel. The smaller member sizes are more favoured by architects. High strength steel represents limited deformability. In this study the deformation of the connection is mainly caused by the deformation of the end-plate and elongation of the bolts. A series of finite element investigation was conducted to study the high strength steel extended end-plate moment connections subjected to monotonic loading. The finite element model of connection is calibrated by using experimental test results of extended end-plate connections.

The steel grade of plate and bolts and the thickness of the plate were changed to investigate the behaviour of the connection. The finite element analysis results demonstrate that the high strength steel extended end-plate moment connections can be suitable for use in steel moment frame structures. The results indicate that by decreasing the end-plate steel grade the ductility was increased but the moment resistance was decreased. 12.9 grade bolts have less ductility than 10.9 grade bolts and 8.8 grade bolts have more ductility than both 12.9 and 10.9 grade bolts. The thinner end plate showed more ductility and lower moment resistance than the thicker end plate. The results obtained from the finite element modeling indicated that the finite element method is a good choice for estimating the behaviour of end-plate connections.

**Keywords:** High Strength Steel, Extended End-Plate Connections, Finite Element Method, Moment Resistance, Ductility.

## ÖZ

Yapılarda yüksek dayanımlı çelik kullanımının bir avantajı daha hafif bir yapı elde edilmesidir. Bu da daha az çelik kullanımı anlamına gelir. Mimarlar daha küçük ebadlarda çelik elemanları tercih ederler. Yüksek dayanımlı çelik kısıtlı oranda deformasyonu temsil eder.

Bu çalışmadaki kolon-kiriş bağlantısının şekil değiştirmesinin en önemli nedeni, plaka bağlantısındaki şekil değiştirme ve civatadaki aksinel uzamadan kaynaklanmaktadır.

Sonsuz elemanlar metodu kullanılarak yüksek dayanımlı çelikten üretilmiş moment bağlantılarının monotonik olarak yüklenmes üzerine bir dizi araştırma yapılmıştır. Bağlantının sonsuz eleman modelinin kalibrasyonu için başka araştırmacılar tarafından aynı tip bağlantılar için yapılan deney sonuçları kullanılmıştır. etodu kullanılarak oluşturulan bağlantı.

Bağlantının davranışını incelemek için çeşitli bağlantı plaka ve civata çelik sınıfı ve plaka kalınlıkları kullanılmıştır. Sonlu elemanlar kullanılarak yapılan analiz sonuçlarına göre yüksek dayanımlı çelik plakalı moment bağlantılarının moment taşıyan çelik karkas yapılarda kullanılması uygun bulunmuştur.

Elde edilen sonuçlara göre plakalı bağlantıların çelik sınıfını düşürmek çelik esnekliğinin artmasına neden olur, aynı zamanda, moment dayanımının da azalmasına neden olur. Sonuçlara göre 12.9'luk civata 10.9 ve 8.8'lik civatadan daha az sünektir. İnce olan bağlantı plakasının kalın olana oranla daha sünek

davrandığı ve daha düşük moment dayanımı olduğu saptanmıştır. Sonlu elemanlar modellemesinden elde edilen sonuçlar plakalı bağlantıların davranışını incelemeye bu yaklaşımın doğru bir seçim olduğu yönündedir.

**Anahtar Kelimeler:** Yüksek dayanımlı çelik, plakalı bağlantılar, sonlu elemanlar Methodu, Moment bağlantıları, süneklik

## **ACKNOWLEDGMENT**

I gratefully and sincerely acknowledge the invaluable advice, supervision expertise and encouragement of my supervisor, Dr. Murude Çelikağ.

I offer heartfelt thanks to my dearest wife, Negar. I am forever indebted to her for her understanding, endless patience, encouragement, support and sacrifice when it was most required.

I wish to thank my parents. Their love and encouragement often provided the most needed motivation to go through the hard times. They have been the most supportive parents a person could ask for. Throughout my life, they have always been my foundation and unwavering in their belief of what I am capable.

To my father in law and mother in law, thank you for believing in my abilities and helping me along every step of the way.

I would like to say thanks to my brother and his wife for their support and guidance over the years.

*This dissertation is dedicated to my lovely wife Negar with love and admiration and to my family especially my father with thanks and appreciation.*

# TABLE OF CONTENTS

ABSTRACT .....	iii
ÖZ .....	iv
ACKNOWLEDGMENT .....	vi
LIST OF FIGURES .....	xi
LIST OF TABLES .....	xiv
LIST OF EQUATIONS .....	xv
1 INTRODUCTION .....	1
1.1 General Introduction .....	1
1.2 Scope of the Study .....	4
1.3 Limitations of the Study .....	4
1.4 Outline .....	4
2 LITERATURE REVIEW .....	6
2.1 Introduction .....	6
2.2 Early Extended End-Plate Models .....	6
2.3 T-Stub Models .....	10
2.4 End-Plate Connection Studies .....	18
3 METHODOLOGY .....	21
3.1. Introduction .....	21
3.2 Connection Classification .....	21
3.2.1 Stiffness .....	21
3.2.2 Strength .....	24
3.2.3 Ductility .....	26
3.3 Types of Partially Restrained Connections .....	26



3.3.1 Single Web-Angle and Single Plate Connections .....	26
3.3.2 Double Web-Angle Connections .....	27
3.3.3 Top and Seat Angle Connections .....	27
3.3.4 Top and Seat Angle with Double Web-Angle Connections .....	27
3.3.5 End-Plate Connections.....	27
3.4 Moment-Rotation Curve.....	34
4 EXPERIMENTAL AND FINITE ELEMENT STUDY .....	39
4.1 Introduction.....	39
4.2 Experimental Tests .....	39
4.3 Details of Finite Element Models .....	42
4.4 Finite Element Modeling.....	43
4.4.1 Symmetric Modeling .....	45
4.4.2 Material.....	46
4.4.3 Bolt Pretension .....	48
4.4.4 Interface Modeling .....	49
4.4.5 Consideration of Friction .....	50
4.4.6 Meshing .....	52
4.4.7 Coupling.....	53
4.4.8 Dynamic Analysis .....	54
5 RESULTS AND DISCUSSIONS.....	57
5.1 Introduction.....	57
5.2 Finite Element Results.....	57
5.3 Comparison of Results .....	70
6 CONCLUSIONS .....	76
6.1 Summary.....	76

6.2 Conclusions.....	76
6.3 Recommendation for Further Study.....	78
REFERENCES.....	79

## LIST OF FIGURES

Figure 1: Sherbourne's End-Plate Joint Model.....	7
Figure 2: Yield-Line Mechanism Employed in Surtees and Mann's Models .....	9
Figure 3: The T-Stub Analogy for Extended End-Plates.....	11
Figure 4: Conceptualizing a T-stub as a Simply Supported Beam.....	11
Figure 5: T-Stub Failure Modes .....	13
Figure 6: Zoetemeijer's Column Flange Collapse Mechanisms.....	14
Figure 7: Classification of the connection by stiffness.....	22
Figure 8: Different zones for classification by stiffness .....	22
Figure 9: Classification of the connection by strength .....	24
Figure 10: Types of End-Plate Beam to Column Connections .....	28
Figure 11: Moment-Rotation Curves for Different Connections .....	30
Figure 12: The Modes of T-Stub Failure .....	32
Figure 13: The Modes of Connection Failure .....	33
Figure 14: Beam to Column Joint Detail .....	34
Figure 15: Moment-Rotation Curve of a Joint .....	35
Figure 16: The Rotation of the Beam and Column under the Couple Forces $Fb$ .....	35
Figure 17: Locations of the Reference Points for Beam and Column.....	36
Figure 18: Position of the Reference Points to Determine the Displacement of the Beam and Column .....	36
Figure 19: The Geometry of the Joint.....	37
Figure 20: Geometry of the Extended End-Plate Connection.....	40
Figure 21: Test Setup in Experimental Test.....	41
Figure 22: The Supports in 3D Simulation .....	42

Figure 23: Symmetric Modeling of an End-Plate Connection .....	46
Figure 24: The Contact between Beam and Plate.....	50
Figure 25: Contact between Different Components of the Connection.....	51
Figure 26: Detail of the Mesh Model of the Joint .....	53
Figure 27: Coupling Point for Reference-Point 1.....	54
Figure 28: Comparison between Implicit and Explicit .....	56
Figure 29: Specimen P10-S690-B8.8 .....	58
Figure 30: Moment-Rotation Curvature for Specimen P10-S690-B8.8 .....	59
Figure 31: Specimen P10-S355-B8.8 .....	60
Figure 32: Moment-Rotation Curvature for Specimen P10-S355-B8.8 .....	60
Figure 33: Specimen P10-S275-B8.8 .....	61
Figure 34: Moment-Rotation Curvature for Specimen P10-S275-B8.8 .....	61
Figure 35: Specimen P10-S690-B10.9 .....	62
Figure 36: Moment-Rotation Curvature for Specimen P10-S690-B10.9 .....	62
Figure 37: Specimen P10-S690-B12.9 .....	63
Figure 38: Moment-Rotation Curvature for Specimen P10-S690-B12.9 .....	63
Figure 39: Specimen P15-S690-B12.9 .....	64
Figure 40: Moment-Rotation Curvature for Specimen P15-S690-B12.9 .....	64
Figure 41: Specimen P15-S355-B12.9 .....	65
Figure 42: Moment-Rotation Curvature for Specimen P15-S355-B12.9 .....	66
Figure 43: Specimen P15-S275-B12.9 .....	66
Figure 44: Moment-Rotation Curvature for Specimen P15-S275-B12.9 .....	67
Figure 45: Specimen P15-S690-B10.9 .....	68
Figure 46: Moment-Rotation Curvature for Specimen P15-S690-B10.9 .....	68
Figure 47: Specimen P15-S690-B8.8 .....	69

Figure 48: Moment-Rotation Curvature for Specimen P15-S690-B8.8 .....	69
Figure 49: Comparison between Finite Element Model and Experimental Test .....	70
Figure 50: Comparison between Experimental and Finite Element Result of P10-S690-B8.8.....	71
Figure 51: Comparison between Experimental and Finite Element Result of P15-S690-B12.9.....	71
Figure 52: Comparison between 10 mm and 15 mm End-Plates with 8.8 Bolt Grades and Same End-Plate Steel Grade .....	72
Figure 53: Comparison between 10 mm and 15 mm End-Plates with 12.9 Bolt Grades and Same End-Plate Steel Grade .....	72
Figure 54: Comparison between End-Plates with Different Steel Grades and Same End-Plate Thickness (10 mm) and Bolt Grade 8.8 .....	73
Figure 55: Comparison between End-Plates with Different Steel Grades and Same End-Plate Thickness (15 mm) and Bolt Grade 12.9 .....	73
Figure 56: Comparison between End-Plates with Different Bolts Grades and Same End-Plate Thickness (10 mm) and End-Plate Grade S690 .....	74
Figure 57: Comparison between End-Plates with Different Bolts Grades and Same End-Plate Thickness (15 mm) and End-Plate Grade S690 .....	75

## LIST OF TABLES

Table 1: Details of the specimens (Girao Coelho & Bijlaard, 2007).....	40
Table 2: Dimensions of the joint .....	43
Table 3: Mechanical properties of the structural steel .....	48
Table 4: Various elements used in ABAQUS (ABAQUS inc, 2006) .....	52
Table 5: Maximum bending moment and maximum connection rotation results .....	58

## LIST OF EQUATIONS

Equation 1 .....	7
Equation 2 .....	8
Equation 3 .....	8
Equation 4 .....	10
Equation 5 .....	10
Equation 6 .....	12
Equation 7 .....	16
Equation 8 .....	16
Equation 9 .....	17
Equation 10.....	17
Equation 11.....	18
Equation 12.....	34
Equation 13.....	34
Equation 14.....	35
Equation 15.....	37
Equation 16.....	37
Equation 17.....	37
Equation 18.....	38
Equation 19.....	38
Equation 20.....	47
Equation 21.....	47
Equation 22.....	47
Equation 23.....	49

# Chapter 1

## INTRODUCTION

### 1.1 General Introduction

The behaviour of steel framed structures extremely depends on the behaviour of beam to column connections. Structural engineers have carried out many researches on the behaviour of structural joints particularly bolted and welded connection, so far. The research findings show that connections have distinctively nonlinear behaviour. This is mainly due to the fact that a connection is a collection of different components and interaction between these components is complex.

Connections in steel frame buildings have to transfer loads from slabs to beams and then to columns. The forces transferred to the joints can be shear and axial forces, torsion and bending moments. In most cases the deformations caused by bending is more important.

The behaviour of beam-to-column moment-resisting joints in steel-framed buildings is represented by a  $M-\Phi$  curve (moment vs. rotation). This curve describes the relation between rotation  $\Phi$  and bending moment  $M$ . This curve describes three main properties: the rotational stiffness, rotation capacity and moment resistance.

Moment-resisting connections have been designed for stiffness and strength with little attention to rotational capacity. In recent years, civil engineers became aware of



the importance of rotational capacity, particularly for earthquake design, and intense research is taking place on this matter to better understand the effect of rotational capacity of joints on the overall behaviour of steel framed structures.

Eurocode 3 classifies connections according to their stiffness and strength. Each classification is further divided into three groups. Connection stiffness is divided as rigid, semi-rigid and, nominally pinned and connection strength as full strength, partial strength and nominally pinned.

End-plate bolted connections are generally considered as semi-rigid and partial strength category and this type of connection is widely used in steel framed buildings. In Europe, extended end-plate connections are generally used for low-rise buildings. This type of connection is popular since, some parts of it can be welded at the fabrication shop and the plate will be bolted to the column on site. There are some design specifications such as Eurocode 3, for the prediction of stiffness and strength of this type of connection but there are no rules for characterization of the ductility of this joint.

One of the main goals of this research is characterization of the rotational behaviour of extended end-plate connection in steel framed structures. The main deformation of this connection often happens in the tension zone.

Before the Northridge (1994) and Kobe (1995) earthquakes the designers and design codes have used forces due to earthquake motions to design welded connections. This approach caused, large moments at connections. However, these connections failed in brittle mode after reaching their capacities. This caused serious damage to

buildings in the earthquake (Mahin, 1998) (Hiroshi, 2000). One important lesson learned from these earthquakes was that the moment capacity is not the only factor affecting the design of steel connections in steel structures. With sufficient moment capacity the connection need to have energy dissipation capacities in ductile mode to resist earthquake forces too.

Seismic and steel structure design codes established some new rules for steel connections after Northridge and Kobe earthquakes. Recently semi-rigid connections or partially restrained connections are also added to design codes and these connections are recognized as economical connections with better performance in steel structures against earthquake than other connection types (Weynand, Jaspart, & Steenhuis, 1998).

There is not enough experimental and analytical research on the seismic behaviour of these types of connections. Therefore, researchers can not characterize moment-rotation curve for different types of connections.

Using high strength steel (HSS) in the steel structures become an important topic in these days. The advantage and disadvantage of high strength steel members was investigated by Galambos et al. (1997). By using the HSS members the size of the sections decrease, resulting in the reduction of the weight of structures and the reduction of transportation and erection cost. If the members become lighter and thinner the foundation of the structure can be smaller and more interior space can be created which is favoured by architects. By using the HSS members the steel consumption can be reduced. When the strength of the steel increase the buckling characteristic of the connection become more important factor. The behaviour of the

high strength steel connections need more study in order to set up a trust worthy design for these types of connections.

In this research ABAQUS software is used to obtain moment-rotation curves to show the effect of nonlinearity in the high strength steel connection. Furthermore, effects of various parameters on the high strength steel connection behaviour are investigated by using the finite element program.

## **1.2 Scope of the Study**

The general aim of the study was to investigate the ductile behaviour of the high strength steel extended end-plate connection. The parameters investigated in this research were the end-plate thickness and steel grade of the end-plate and bolts.

## **1.3 Limitations of the Study**

This research has some limitations. This research only focused on the extended end-plate connection. The geometry of the specimens was same having four tension bolts and two shear bolts. There was also limitation for the steel grade for the column and the beam. The steel grade for these members were S355. This study was limited to the investigation of the behaviour of the connection under monotonic loading and the effect of the temperature was not considered in this research.

## **1.4 Outline**

This thesis is structured as follows:

Chapter I is the general introduction to the concept of this research and the limitations that faced in the process of the study.

Chapter II presents the theories by others for the prediction of the behaviour of the end-plate connections. This chapter focuses on the early extended end-plate investigations and t-stub models and related studies on the end-plate connections.

In Chapter III the classification of the joints according to Eurocode 3 was illustrated and the steps for drawing the moment rotation curve were explained. The moment rotation curve describes the rotation between the components and the bending moment that applied to the joint.

Chapter IV represents the experimental tests that used to verify the finite element part of this research and all details about finite element simulation of this study.

Chapter V contains the result of the finite element analysis of the high strength extended end-plate connections and compares the result with each other to understand the behaviour of the connection under variation of the end-plate thickness and steel grade of the end-plate and bolts.

In Chapter VI presents the conclusions of this thesis and the future study was explained. This chapter is followed by bibliography.

## Chapter 2

### LITERATURE REVIEW

#### 2.1 Introduction

Many theories have been proposed to predict the behaviour of the end-plate connections. This literature covers a wide variety of such theories. This chapter will focus on the early extended end-plate investigations and t-stub models and related studies on the end-plate connections.

#### 2.2 Early Extended End-Plate Models

Sherbourne (1961) shown a model of extended end-plate connection, and he investigated the context of the global plastic analysis of a frame and if connection fail plastically at the same time of failure of the beam it will be optimum economy assumption for the connection. And Sherbourne wants to design a ductile and full-strength extended end-plate connection.

Sherbourne tested five different extended end-plate connections with thickness varying from approximately 19 mm to 32 mm. The bolt and stiffener sizes were different. In his modeling the end-plate behave as a fixed ended beam spanning from the flush bolt line to the extended bolt line as shown in Figure 1, and load was applied at beam tension flange.

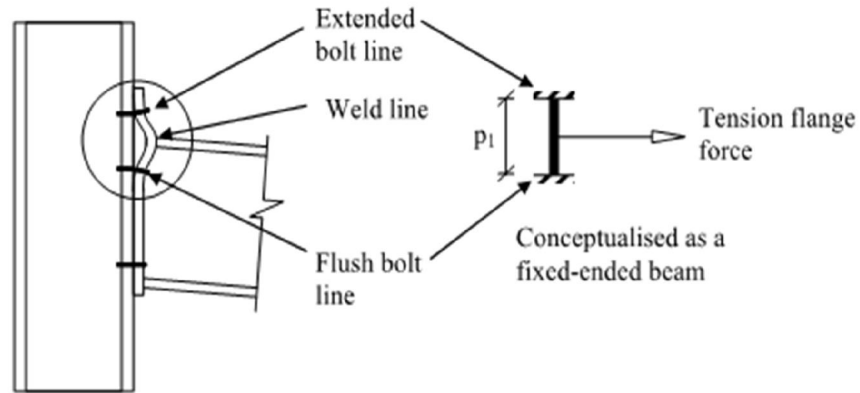


Figure 1: Sherbourne's End-Plate Joint Model  
(Source: Sherbourne, 1961)

For this fixed ended beam, he assumed a plastic collapse with plastic hinges at the weld line at the end-plate to beam flange and at the flush and extended bolt lines.

The resulting equation is as follows:

$$f_y b t_f \frac{p_1}{8} = \frac{b_p t_p^2}{4} \sqrt{f_y^2 - \frac{3f_y^2}{4} \left[ \frac{b t_f}{b_p t_p} \right]^2} \quad (\text{Equation 1})$$

$p_1$  : the bolt pitch

$b_p$  : the endplate width

$t_p$  : the endplate thickness

$b$  : the breadth of the beam flange

$t_f$  : the thickness of the beam flange

$f_y$  : the material yield stress for both the beam flange and endplate

The left side of the equation shows the force needed to cause yielding of the beam tension flange. It also represents the theoretical collapse load for a fixed ended beam with tension flange force as a central force and with span  $p_1$ . The right side of the

equation shows the moment that modified for shear to cause plastic collapse of the end-plate across the breadth.

The equation can be simplified if  $f_y$  on the left side of equation (the beam flange yield stress) is taken equal to  $f_y$  on the right side of equation (the end-plate yield stress).

$$\left[ \frac{bt_f}{b_p t_p} \right]^2 \left[ \left( \frac{p_1}{2t_p} \right)^2 + \frac{3}{4} \right] = 1 \quad \text{(Equation 2)}$$

Assumptions for calculating the bolt thread area  $A_s$  :

- The bolts are assumed to restrain the end-plate completely on either side of tension flange.
- The bolts are fully loaded (proof or yield load) and equally stressed at the same time as the beam tension flange.

$$A_s = \frac{bt_f}{4} \cdot \frac{f_y}{f_{yb}} \quad \text{(Equation 3)}$$

$f_{yb}$  : the proof stress for the bolts

Sherbourne's one dimensional plastic model for both the extended and flush regions is shown in Figure 5. Meanwhile the behaviour of both flush and extended regions is the same in this model, the end-plate tension area is assumed as a t-stub and the stiffening effect is ignored for the beam web. Sherbourne used thin end-plates in his experiments and he noted that the tension bolts in extended region may attract fewer loads than the bolts in the flush region. However, he did not consider this in the formula and he did not mention of prying forces in the bolts.

According to the need for full strength connection, Sherbourne found that plastic failure of the connection is the important value of designing and he believe the connection should developed to achieve adequate ductility, however he did not consider to predict the rotation capacity.

Surtees and Mann (1970) tested six single side extended end-plate connection with different end-plate thickness at the University of Leeds. In one of the tests they used different pretension for bolts and they concluded that the applied pretension on the bolts has effect on the initial stiffness of the connection.

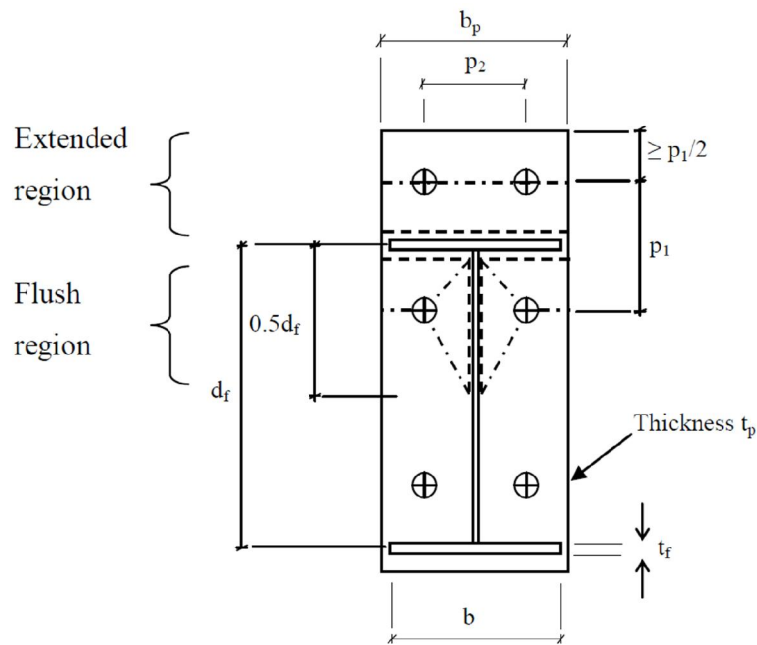


Figure 2: Yield-Line Mechanism Employed in Surtees and Mann's Models  
(Source: Surtees and Mann, 1970)

The Surtees and Mann (1970) yield line mechanism is shown in Figure 2. The yield lines are in two regions, the first region is the extended region and second one is in the flush region. The assumption for the extended region is the same as the assumption of Sherbourne (1961), and the extended bolts assumed to restrain the



end-plate completely, but he considered that bending occurred across the end-plate due to existence of the web.

Their assumption was that the yield lines for flush region appear in a distance equal to  $0.5d_f$  in the extended region and, as shown in Figure 2. They suggested equations for the calculation of the bolt size and end-plate thickness.

Surtees and Mann (1970) end-plate thickness equation is given in Equation 4:

$$t_p = \sqrt{\left(\frac{M_p}{16d_f \left[\frac{2b_p}{p_1} + \frac{d_f}{p_2}\right]}\right)} \quad \text{(Equation 4)}$$

$d_f$  : is the depth between centers of the beam flanges

$p_2$  : the bolt gauge distance

Surtees & Mann considered effect of prying action in the connection and for this reason they increased the bolt load by 30% and design the bolts sizes according to force P.

$$P = \frac{M_p}{4d_f} \cdot 1.3 \approx \frac{M_p}{3d_f} \quad \text{(Equation 5)}$$

Surtees and Mann (1970) established 0.03 radians rotation is a suitable value for the plastic rotation of connection.

### 2.3 T-Stub Models

In extended end-plate connection, the column flange and the extended part of end-plate is assumed to behave like T profile as shown in Figure 3.

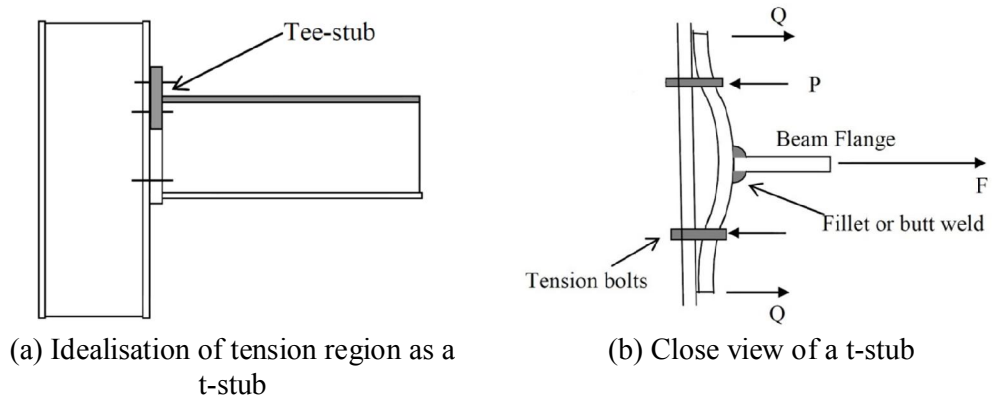


Figure 3: The T-Stub Analogy for Extended End-Plates

Douty and McGuire (1965) had investigation into tee stub in end-plate connections at Cornell University in United State. They identified that the behaviour of the tension part and tee stub in extended end-plate connection are similar, and with this model they compute the prying force in the extended bolts. The computation of the prying forces was based on the initial bolt elongations and the initial elastic deformation of the endplate that appear around the bolts because of the bolt pretension. They assumed the tee stub as a simply supported elastic beam as shown in Figure 4.

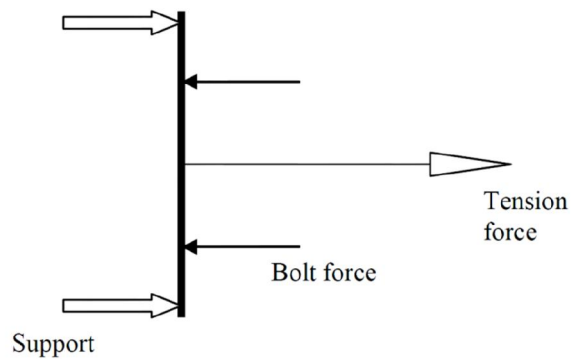


Figure 4: Conceptualizing a T-stub as a Simply Supported Beam

The equation by Douty and McGuire (1965) for the semi-empirical prying force  $Q$  at ultimate load is given in equation 6:

$$Q = \left[ \frac{\frac{1}{2} - \frac{b_p t_p^4}{30 e_x m_x^2 A_s}}{\frac{e_x}{m_x} \left( \frac{e_x}{3m_x} + 1 \right) + \frac{b_p t_p^4}{6 e_x m_x^2 A_s}} \right] F_u = K_2 F_u \quad (\text{Equation 6})$$

$Q$  : Praying force

$b_p$  : Width of the end-plate

$t_p$  : Thickness of the end-plate

$e_x$  : The end distance for the extended bolt row

$m_x$  : The effective distance between the weld line and the extended bolts

$A_s$  : The bolt effective area

$F_u$  : The ultimate force in the beam flange

The total bolt forces were checked by calculating the praying forces for extended part of the end-plate and certifying that the failure of the connection is not due to the bolt fracture.

The maximum bending stress should not be more than the value of  $4M_p / t_p^2$  ( $M_p$  : The maximum plate moment) to certify the thickness of the tee stub flange or the end-plate. The bending moment  $M$  is chosen between the higher bending moment at the weld line or at the bolt line.

The moment at the weld line was calculated by taking moment for  $Q$  and total force about the weld line and the bolt line moment was calculated by taking moment for  $Q$  about the bolt line.

Douty and McGuire (1965) recognized two types of failure modes for tee stubs, in the first failure mode the end-plate separated from column flange before yielding of the end-plate and in second failure mode yielding will appear before the end-plate separated from column flange as shown in Figure 5. The first mode of failure will appear in extended end-plate connection with thick end-plate and the second one will appear in connection with thin end-plate.

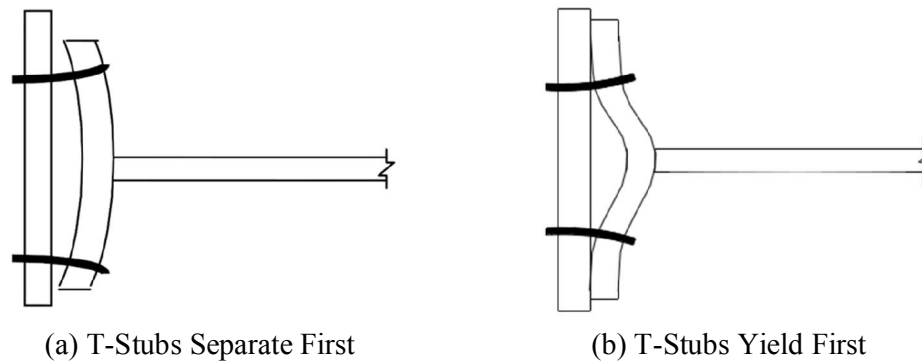


Figure 5: T-Stub Failure Modes  
(Source: Douty & McGuire, 1965)

Nair et al. (1974) investigated that the prying action is one of the important factors in the behaviour of tee stubs and they found that changes in the end distance and the bolt pitch have effect on prying action.

Zoetemeijer (1974) modeled one-dimensional tee stub idealized as simply supported beam, in his collapse analysis where a plastic hinge was at the weld line and another plastic hinge was at the bolt line. He mentioned two failure modes in his model, the first one was when the mechanism failed by fracture of the bolts and in second mode was when extreme deformation of the t-stub flange. Causes failure and through the formation of plastic hinges. He concluded that it is possible to control the failure mode by varying the size of the bolt and the thickness of the plate.

He also considered two collapse mechanisms for column flange. First mechanism was caused by bolt fracture, and second one was caused by extreme deformation of the column flange. These two types of collapse mechanisms are shown in Figure 6.

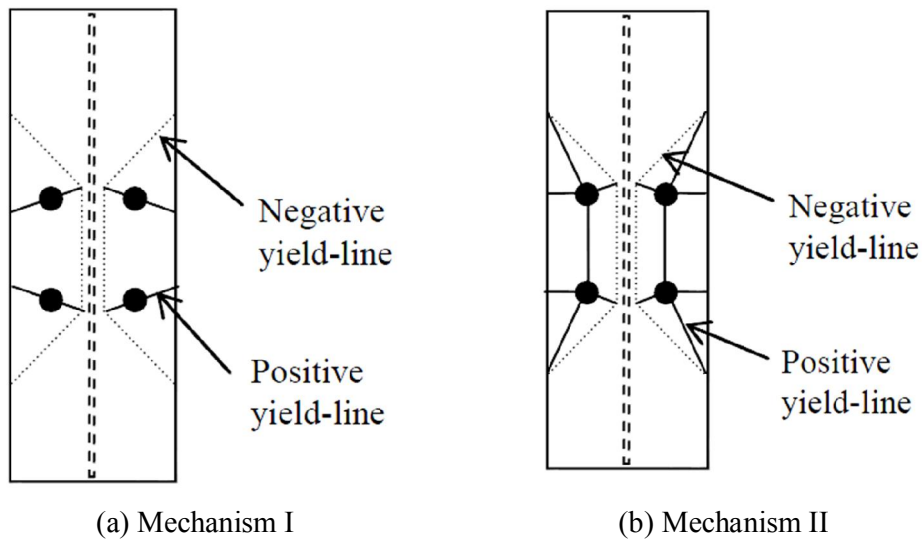


Figure 6: Zoetemeijer's Column Flange Collapse Mechanisms  
(Source: Zoetemeijer, 1974)

He demonstrated the effect of thin and thick end-plate, strength and bolt size on the behaviour of the connection and he found that for larger deformations of the thin end-plate the connection requires larger and stronger bolts.

Model of Packer and Morris (1977) was similar to model of Zoetemeijer and their research was on deformation of the column flange. They assumed that the shear deformation in their model is negligible. They presented their own three collapse mechanisms. The first one was for thick tee stubs, where there was no yielding in the tee stub and the failure was caused by fracture in bolts.

In the second mechanism, yielding of the tee stub flange was only along the weld line, and in the last mechanism yielding of the tee stub flange was happened in both bolt line and weld line.

In their models that were failed by third mechanism they found different behaviour for same failure mechanism. They used Zoetemeijer's equation to predict the connection strength for the extended end-plate. However they found that the Zoetemeijer equation overestimates the connection strength for the extended end-plate connection. The equation underestimates the connection strength for t-stub for this reason they demonstrate that the behaviour of the end-plate was not similar to tee stub in thin end-plate connections.

The earlier work was continued with Phillips and Packer (1981). They presented that the end-plate thickness has effect on failure mechanism and it has moment-rotation characteristics.

Kennedy et al. (1981) focused on "split tee analogy" they found similarity between extended and tee stub region. The three types of failures that they were used in their analysis were the mechanisms that Packer and Morris (1977) were considered. The thin end-plate fails due to yielding at the bolt and weld line and for the thick end-plate the failure is caused by fracture in the bolts. There was no prying force in this type of end-plate, and for end-plates with thicknesses between thin and thick (intermediate end-plate) the failure happened because of fracture in bolts and yielding was only in the weld line.

Their model demonstrated that the geometry of the end-plate is very important factor on the behaviour of the end-plate connection and failure mechanism.

They also illustrate that the connection behaviour is similar to the behaviour of the thick end-plate connection when  $t_1$  is the end-plate thickness:

$$t_1 = \sqrt{\frac{2bt_f f_{yf} p_f}{b_p \sqrt{f_y^2 - 3\left(\frac{bt_f}{2b_p t_1} f_{yf}\right)^2}}} \approx \sqrt{2.11 * p_f t_f \cdot \frac{b}{b_p} \cdot \frac{f_{yf}}{f_y}} \quad (\text{Equation 7})$$

$b$  : width of the beam flange;

$t_f$  : thickness of the beam flange;

$f_{yf}$  : yield stress of the beam flange;

$b_p$  : width of the end-plate

$f_y$  : yield stress of the end-plate

$p_f$  : the distance from the face of the beam flange to the bolt line

The beam flange force is set at its elastic limit  $F_{max}$  where:

$$F_{mx} = \frac{bt_f f_{yf}}{2} \quad (\text{Equation 8})$$

When the end-plate thickness is more than  $t_1$ , the yielding of the end-plate cannot take place before the beam flange force exceeds  $F_{max}$ . In this situation there is no any prying force. Q is equal to zero and this failure mode is thick end-plate failure mechanism.

Also they concluded that the behaviour of the connection is similar to the behavior of a thin end-plate connection when  $t_{11}$  is the end-plate thickness:

$$t_{11} = \sqrt{\frac{2(bt_f f_{yf} p_f - \frac{\pi}{16} d_b^3 f_{yb})}{b_p \sqrt{f_y^2 - 3[\frac{bt_f}{2b_p t_{11}} f_{yf}]^2} + b_p \sqrt{f_y^2 - 3[\frac{bf_t}{2b_p t_{11}} f_{yf}]^2}}} \approx \sqrt{\frac{2(bt_f f_{yf} p_f - \frac{\pi}{16} d_b^3 f_{yb})}{(0.85b_p + 0.8b_p) f_y}} \quad (\text{Equation 9})$$

$d_b$  : the bolt diameter

$b_p$  : (the endplate width) – (the bolt hole diameter)

The end-plate is thin when the end-plate thickness is less than  $t_{11}$ , and at ultimate load, the praying force is maximum value.

$$Q_{max} = \frac{b_p t_p^2}{4e_x} \sqrt{f_y^2 - 3\left(\frac{F}{b_p t_p}\right)^2} \quad (\text{Equation 10})$$

$t_p$  : end-plate thickness

$Q_{max}$  : the maximum value of praying force

$e_x$  : the edge distance from the bolt line to the end-plate edge

$F$  : the flange force which has its maximum at the elastic limit as  $F_{max}$

A limit was set on the value of  $e_x$ , that limit is  $2d_b \leq e_x \leq 3d_b$ .

For intermediate plate, the thickness of plate is between  $t_1$  and  $t_{11}$ , when  $F$  is equal to

$F_{max}$ , the maximum value of the reduced praying force  $Q'_{max}$  will be.



$$-Q'_{max} = \frac{b_p t_p^2}{4e_x} \sqrt{f_y^2 - 3\left(\frac{F_{max}}{b_p t_p}\right)^2} + \frac{\pi d_b^3}{32e_x} f_{yb} - \frac{F_{max} p_f}{e_x} \quad (\text{Equation 11})$$

For ductile behaviour the bolts are sized to be stronger than  $(F + Q')$ <sub>max</sub> .

Sherbourne and Mohammad (1994) used 3D finite element modeling to draw moment-rotation curvature for steel connection. They used ANSYS package for their modeling. They suggested a method to estimate the stiffness of the connection. Their model involve plate, beam and column and they also modeled bolt shank, nuts, and interaction between component but pre stressing for the bolts was not included.

They presented the behaviour of the connection including failure which can be correctly modeled by 3D finite element modeling. Meng (1996) modeled extended endplate connection under cyclic loading.

Kukreti et al. (1987) demonstrated a method for a steel bolted end-plate connection to develop the moment-rotation relationship. They used finite element method to analyze the connections with different geometry and assess the behaviour of the end-plate and predict the maximum end-plate separation. The analytical part has been validated by comparing with experimental test result of some specimens.

## 2.4 End-Plate Connection Studies

Sumner et al. (2000) tested eight bolt extended stiffened and four bolted extended unstiffened end-plate connections and used finite element method as a validation study. Their research shown eight bolt extended stiffened and four bolted extended unstiffened end-plate connections are suitable to withstand against cyclic loading.

They demonstrated that the end-plate connections with strong plate are more ductile than the weak plate connections and the weak plate connections failed in brittle manner and they presented that for designing the connection the effect of slab should be considered.

The maximum moment strength of the end-plate connection that predict by Eurocode 3 is very conservative than the experimental result (Yorgun, 2002).

The effect of the end-plate thickness on the behaviour of the connections, in thin end-plate connection the plastic deformation of the end-plate in bending is most important factor on the behaviour of the connection, when the thickness of the end-plate increase, the flexural resistance with respect to bolt resistance is the important factor and in this type of connection the plastic deformation of the bolts will increase. Coelho et al. (2004) designed the connections to use the full plastic moment capacity of the beam. The steel grade and end-plate thickness were the parameters that they mentioned in their investigations. They demonstrated the flexural strength and stiffness connections will increase by increase the end-plate thickness however rotation capacity will decrease. And the failure modes in their experiments involved nut stripping, weld failure, and bolt fracture. Also they investigated the moment resistance of the connections by increasing the end-plate thickness which will in turn increase the initial rotational stiffness. It was also shown that the steel grade has little effect on these properties. They indicated that when joint resistance is concerned the Eurocode 3 has a safe approach but for the joint initial stiffness the same code over estimates the results.

Tahir and Hussein (2008) investigated eight extended end-plate tests, their parameters were size and number of bolts, thickness and size of end-plate and size of beams and columns. They demonstrated that the end-plate connections with deeper beam have higher initial stiffness. This was due to the longer distance between tension zone and compression zone and it helped to reduce the rotation capacity of the end-plate connection.

The research results by Adey et al. (1998) was the effect of the beam size, bolt layout, end-plate thickness and extension stiffeners on the ability of the end-plate to absorb energy. They evaluated the behaviour of the end-plate and for this reason they designed the end-plate connection with strong column and beam and weak extended end-plate to ensure end-plate failure will happen before yielding of the column and beam. They illustrated that the end-plate connections ductility will reduce by increasing the beam size and also the ability of energy absorption will also decrease. If the bolt layout is changed from a tight bolt configuration to a relaxed bolt configuration then the moment capacity of the connection would decrease and the ductility of the connection will increase.

They presented that a high moment capacity; high energy absorption and good ductility are advantages of stiffened extended end-plate connections.

## Chapter 3

### METHODOLOGY

#### 3.1. Introduction

The ductility is a very important factor in the behaviour of joints. Eurocode 3 (2005) classifies joints only by the stiffness and the strength of the connections and the ductility of connections is not classified. The characteristic behaviour of the connection is represented by the relationship between moment and rotation of the connection. This relationship is presented as moment rotation curve.

#### 3.2 Connection Classification

Joint classification depends on three parameters in Eurocode 3 (2005) as well as in AISC codes (AISC, 2005). These parameters are:

- Stiffness
- Strength
- Ductility

These parameters are explained in the Eurocode 3 as follows:

##### 3.2.1 Stiffness

A connection is classified as a semi rigid, rigid and nominally pinned depending on the initial rotational stiffness  $S_{j,ini}$ . The slope of the moment-rotation curve is equal to  $S_{j,ini}$  where the connection still behaves elastically as it is shown in Figure 7.

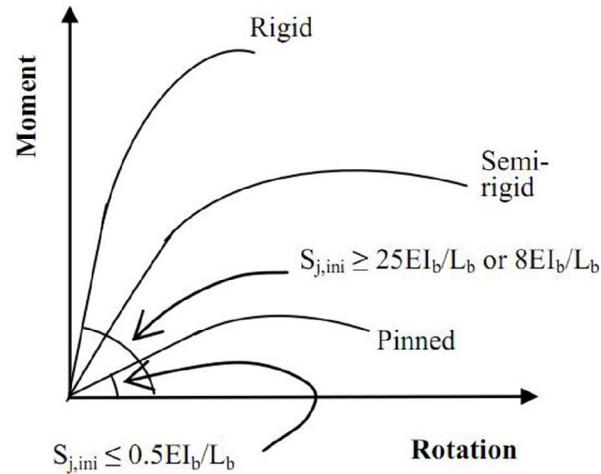


Figure 7: Classification of the connection by stiffness  
(Source: Eurocode 3, 2005)

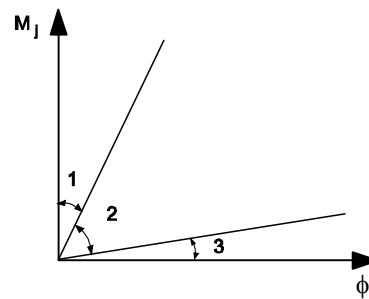


Figure 8: Different zones for classification by stiffness  
(Source: Eurocode 3, 2005)

The moment rotation curve was divided into three zones for classification of the connection by stiffness, as it is shown in Figure 8.

Zone 1: Rigid

For a braced non-sway frame if  $S_{j,ini} \geq 8EI_b / L_b$  the joint is considered as rigid, for an un-braced frame or a sway frame the corresponding limit is  $25EI_b / L_b \cdot L_b$  and  $I_b$  are the beam span and second moment of area respectively. Where the bracing reduces the horizontal displacement by more than 80%, those are non-sway braced frames.

$$\text{If } S_{j,ini} \geq k_b EI_b / L_b$$

where,

$k_b = 8$  for frames where the bracing system reduces the horizontal displacement by at least 80 %

$k_b = 25$  for other frames, provided that in every story  $K_b / K_c \geq 0.1$

Zone 2:        Semi-Rigid

All joints with moment-rotation curves between the limits for pinned and rigid joints are defined as semi-rigid joints.

All joints in zone 2 should be classified as semi-rigid. Optionally, joints in zones 1 or 3 may also be treated as semi-rigid.

Zone 3:        Nominally Pinned

If the initial stiffness  $S_{j,ini} \leq 0.5EI_b / L_b$  a joint is considered to be pinned. This applies to both non-sway and sway frames.

$$\text{If } S_{j,ini} \leq 0.5 EI_b / L_b$$

The joint classified as semi-rigid for frames

where,  $K_b / K_c < 0.1$

$K_b$     is the mean value of  $I_b / L_b$  for all the beams at the top of that story;

$K_c$     is the mean value of  $I_c / L_c$  for all the columns in that story;

$I_b$  is the second moment of area of a beam;

$I_c$  is the second moment of area of a column;

$L_b$  is the span of a beam (Center-to-center of columns);

$L_c$  is the story height of a column.

### 3.2.2 Strength

Connections are grouped as full-strength, partial-strength or nominally pinned when the design moment resistances of the members that it connects with is compared with its design moment resistance  $M_{j,Rd}$ . (Figure 9).

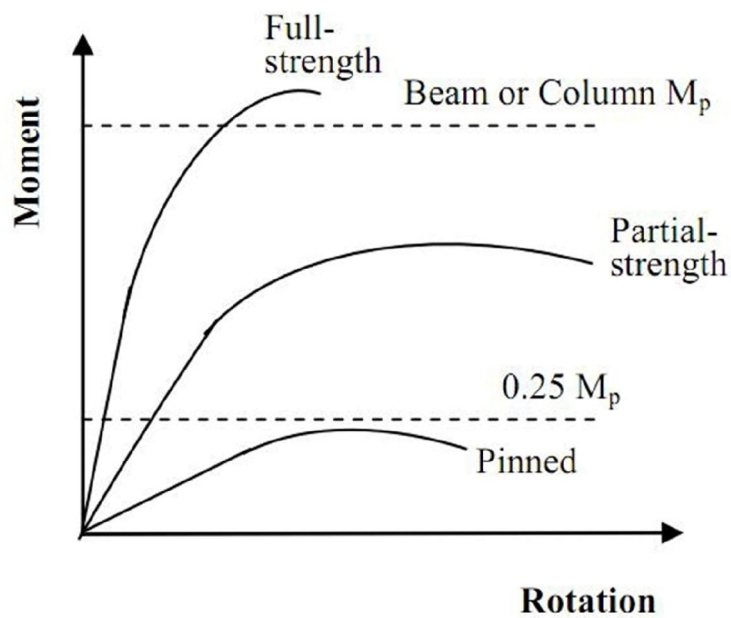
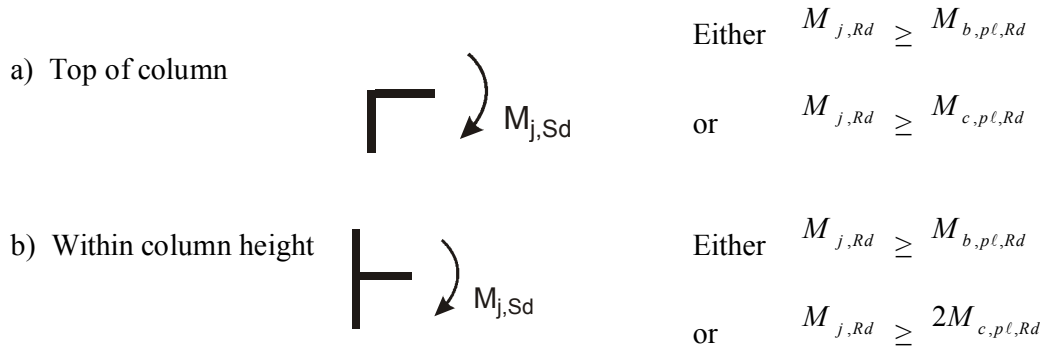


Figure 9: Classification of the connection by strength  
(Source: Eurocode 3, 2005)

### 3.2.2.1 Full Strength Connections



Key:

$M_{b,p\ell,Rd}$  is the design plastic moment resistance of a beam;

$M_{c,p\ell,Rd}$  is the design plastic moment resistance of a column.

The full strength connections should be able to transfer 100 percent of the column design moment to the beam and 100 percent of the beam design moment to the column and the design resistance of the joint shouldn't be less than the resistance of the member. It meets the criteria shown in Figure 9.

### 3.2.2.2 Nominally Pinned Connections

A nominally pinned connection should be able of transmit less than 25 percent of the beam or column design moment or the design moment resistance  $M_{j,Rd}$  should not be grater than 0.25 times the design moment resistance that is needed for a full-strength connection. It should also have adequate rotation capacity.

### 3.2.2.3 Partial Strength Joints

The partial-strength joint is defined as joints falling between those two limits for a nominally pinned joint and a full-strength joint. It should be able to transfer between 100 – 25 percent of the design moment.

The priority shifts from strength to ductility if the beam strength exceeds the connection strength (Chen, 2000).



### 3.2.3 Ductility

The ductility is a typical matter in partial strength connections and a very important parameter when research is focused on the deformation of connections (Chen, 2000).

In Eurocode 3 ductility of connections are not classified. For extended endplate connections it is not possible to calculate the rotation capacity directly. Surtees and Mann (1970) and Bose and Hughes (1995) proposed that a connection is sufficiently ductile if the connection achieved a rotation of 0.03 radians. Connections are grouped as non-ductile if they achieve less than 0.03 radians of rotation.

Following AISC Seismic Provision (2005) if  $\theta_u$  refer to the value of connection rotation at ultimate moment and  $\theta_u^*$  the value of rotation at the point where the moment is within the 80% of the ultimate value.

- If  $\theta_u^* \geq 0.04$  radians, the connection of a special moment frame (SMF) is ductile.
- If  $\theta_u^* \geq 0.02$  radians, the connection in an intermediate moment frame (IMF) is ductile.
- Otherwise connection is considered as brittle.

## 3.3 Types of Partially Restrained Connections

### 3.3.1 Single Web-Angle and Single Plate Connections

The single web-angle connection produced of an angle bolted or welded to both the beam web and the column. The moment rigidity of the single web-angle connection is equal to about one-half of the double web-angle connection. The single web-angle connection has rigidity equal or less than the single plate connection while in the

single plate connection one side of the plate is fully welded to the column flange (Chen, 2000).

### **3.3.2 Double Web-Angle Connections**

The double web-angle connection is made of two angles bolted to both the beam web and the column. The double web-angle connection is in fact stiffer than single web angle connection. But the moment capacity of this type of connection is one of the lowest among the other types.

### **3.3.3 Top and Seat Angle Connections**

The top and seat angle connection is composed of two flange angles, which connects the beam flanges to column flange. The top angle connection is used to present lateral support to the compression flange of the beam and the seat angle connection is used to transfer only the vertical shear and should not give a significant restraining moment at the end of the beam (Chen, 2000).

### **3.3.4 Top and Seat Angle with Double Web-Angle Connections**

The combination of top and seat angle and double web angle produces this type of connection. This type of connection grouped as semi rigid connection (Chen, 2000).

### **3.3.5 End-Plate Connections**

The end-plate connection is formed of an end-plate that is welded to the beam in the workshop and the beam will be bolted to the column on site using the pre-drilled holes of the beam end-plate. In 1960 usage of this type of connection increased (Chen, 2000). The end-plate connections classified into three groups that are shown in Figure 10.

- Extended end-plate connection
- Flush end-plate connection
- Partial depth connection (Header Plate Connection)

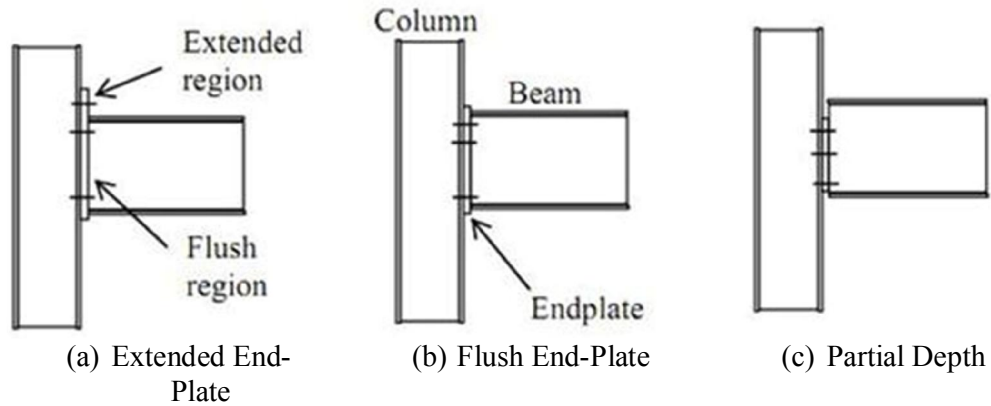


Figure 10: Types of End-Plate Beam to Column Connections

The extended end-plate connection is divided into two groups. First one is extended on the tension side only and second group is extended in both compression and tension sides. Extended end-plate connections can be stiffened or unstiffened, and gusset plate welded to the outside of the beam flange and to the end-plate as stiffener in the stiffened configuration.

Flush end-plate connection: end-plate does not extend beyond the outside of the beam flange and end-plate covers the beam depth and all bolts located inside the flanges. Flush end-plate connections are classified as stiffened or unstiffened, in the stiffened pattern gusset plates are welded on both sides of the end-plate and beam web.

And partial-depth end-plate connection only covers a part of beam depth as displayed in Figure 10c. This type of connection generally categorized as simple connection and it is used to transfer the vertical shear of the beam to the column instead of the beam moment.

Flush end-plate is generally used for the roof construction and this type of end-plate

connection is weaker than the extended end-plate connection. On the other hand, in most of the current design codes one of the important characteristics of extended end-plate connection is its capability of transferring higher moment from beam to column and this reason makes this type of connections fully restrained rather than partially restrained (AISC, 2005) (Eurocode 3, 1997) (Chen, 2000). The behaviour of end-plate connection depends on the column flanges which act to prevent flexural deformation and in that way influence the behaviour of the fasteners and the end-plate (Chen, 2000).

### **3.3.5.1 Extended End-Plate Connection**

An extended end-plate connection consists of a beam that welded to the plate in the fabrication shop, the plate and column face are pre drilled and bolted on the site. In this type of connection the plate extends above the tension flange of the beam. This increases the lever arm of the bolt group and therefore the load carrying capacity of the bolts increase. End-plate connections have more ductility than the beam to column welded connections since the bolted beam to column connections have less rigidity than the welded type of connections. For this type of connection welding is done in fabrication shop. Therefore, it is easier to achieve high quality welding.

Ductility level is one of the important features of the extended end-plate connection. Ductility is synonymous with rotation capacity and it should not be confused with the ductility of the material. Ductility in connections means the capability of acting as a plastic hinge.

Figure 11 shows the moment-rotation curves for six different types of connections (Chen & Kishi, 1989), which demonstrated the non-linear behaviour of the connection over the range of loading. This curve shows that the end-plate connection

considered as part of the partial strength connection group. In this curve x-axis signifies the perfect pinned connection and the y-axis signifies the perfect rigid connection.

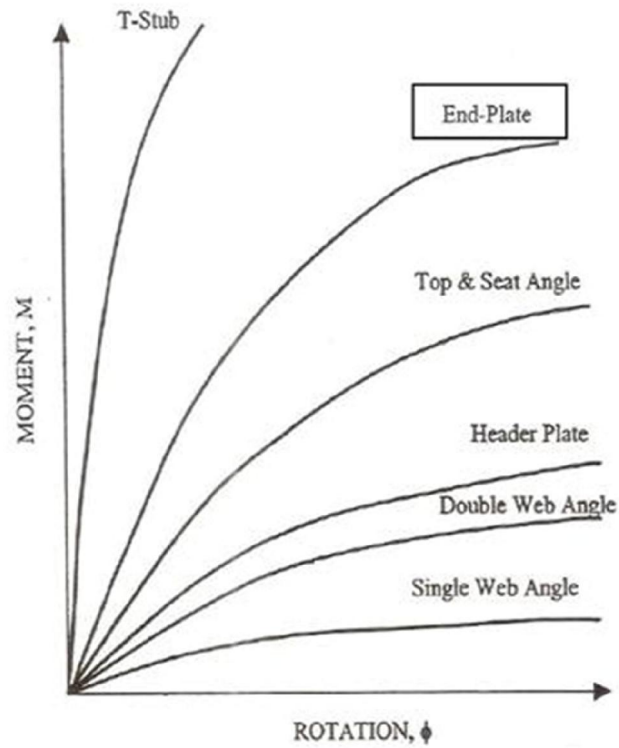


Figure 11: Moment-Rotation Curves for Different Connections  
(Source: Chen & Kishi, 1989)

The following are some of the advantages of end-plate connections:

- 1) This type of connection is suitable for installation in winter because only bolting is needed on the site.
- 2) Welding is good quality and since it is done in fabrication shop then it has minimum problems.
- 3) The installation process is very fast and inexpensive without the need of site welding.

The following are some of the disadvantages of end-plate connections:

- 1) The plate may often warp due to the heat of the welding.
- 2) The bolts are in tension and they may be subject to prying forces.

By using equivalent t-stub for end-plate connections in bending, the yield lines occur around the bolts. Modes of failures divided into three groups: (Eurocode 3, 1992) (SCI, 1995). The modes of t-stub failure are shown in Figure 12.

1) Mode I: Complete flange yielding

The flange is yield but the bolts are not yielded yet. The bolt head has deformation since the strength of the bolt is more than the strength of the flange (Figure 12a).

2) Mode II: Bolt failure with flange yielding

The flange and bolts are yielded together, in mode II the strength of the flange and bolts are equal (Figure 12b).

3) Mode III: Bolt failure

The strength of flange is more than bolts and bolts will yield first (Figure 12c).

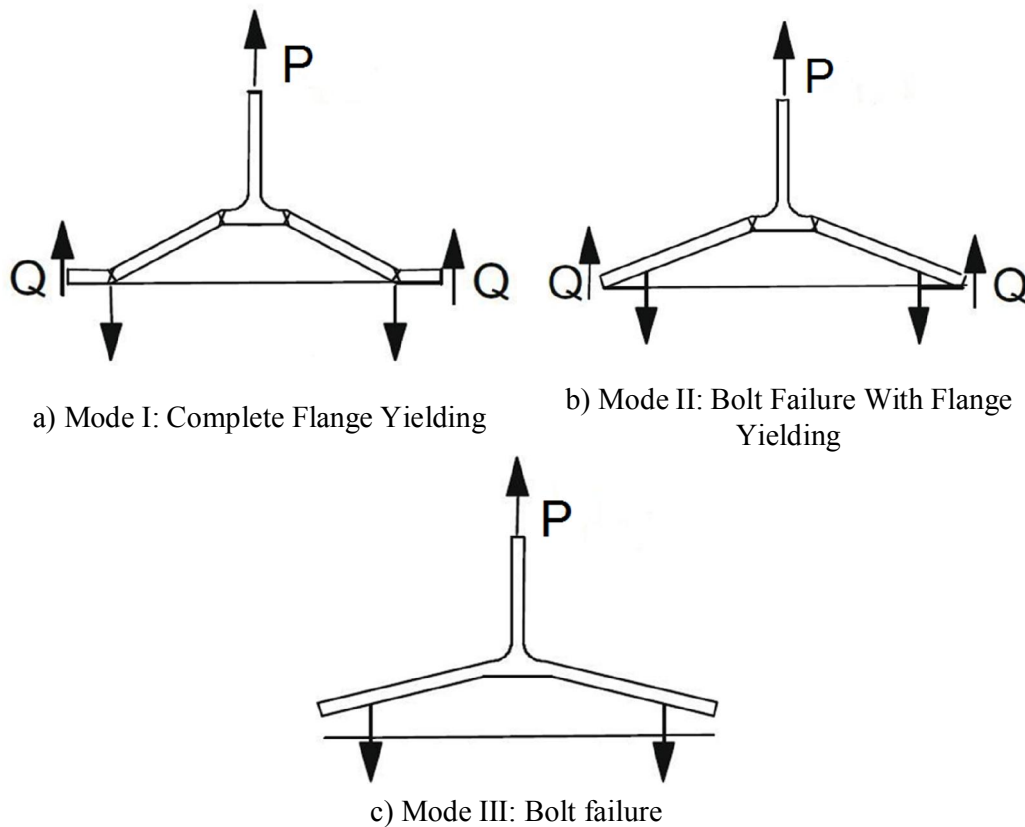


Figure 12: The Modes of T-Stub Failure  
(Source: Eurocode 3, 2005)

Both the experimental test and finite element simulation show similar modes of failure for the end-plate connections. These modes of failure are shown in Figure 13a, b, c.

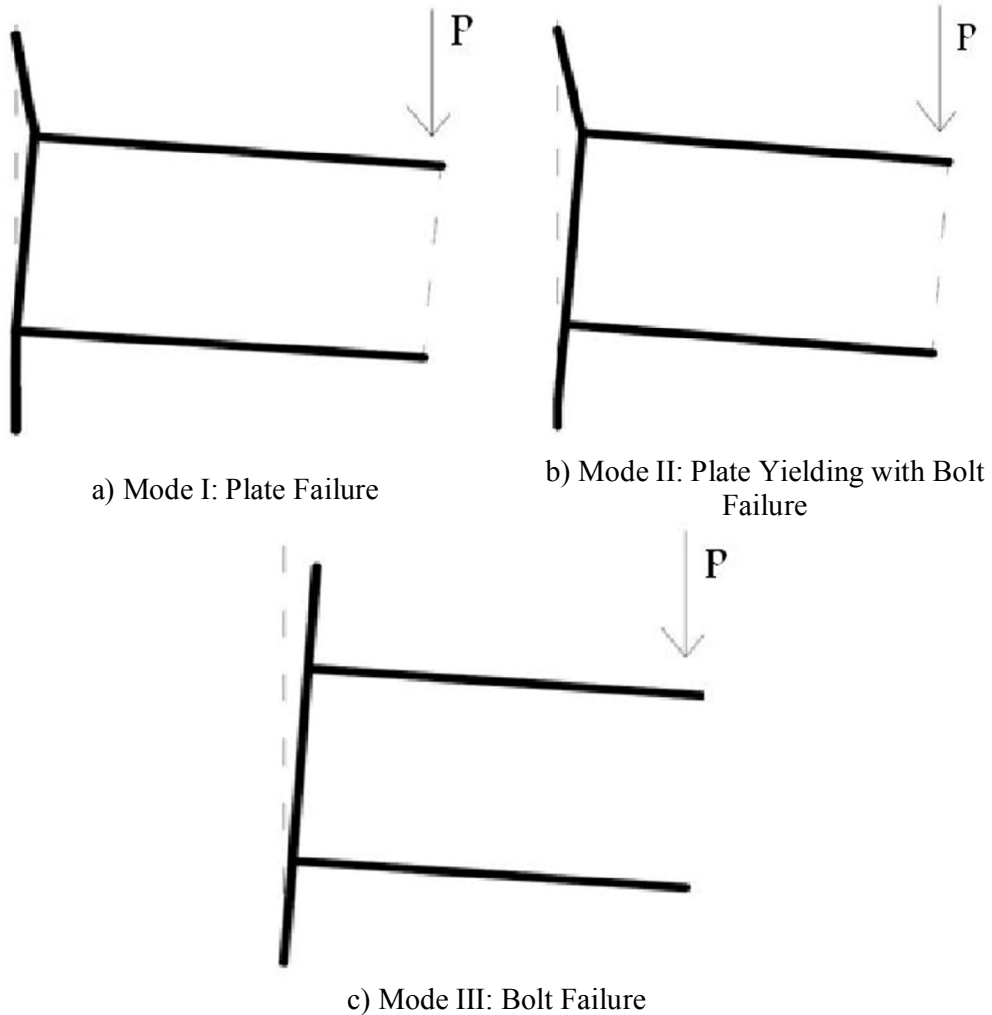


Figure 13: The Modes of Connection Failure



### 3.4 Moment-Rotation Curve

One beam to column joint consists of a web panel and a connection as shown in Figure 14. The web panel zone consists of the flange and web of the column for the height of the connected beam profile. The connection means the location where the two members are interconnected and it includes all the components that fasten to each other.

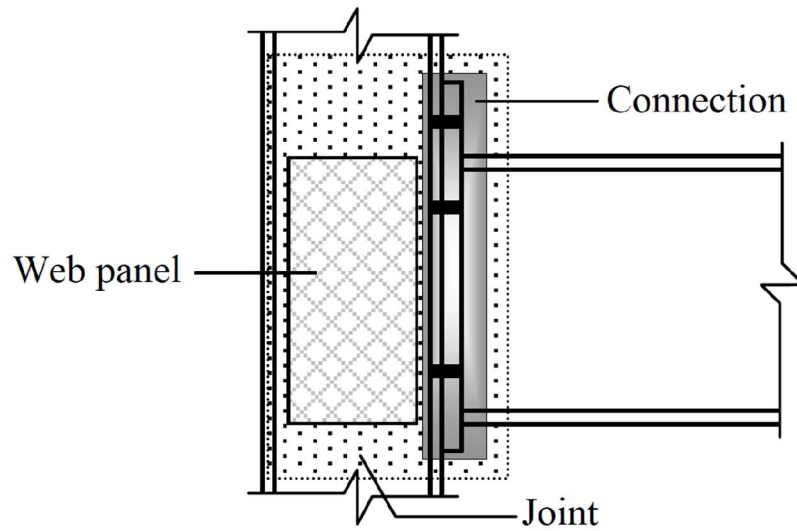


Figure 14: Beam to Column Joint Detail

$M - \Phi$  curve shows the behaviour of the beam to column joint as already explained. The deformation of the connection is caused by deformation of the bolts and end-plate and the deformation of the column web. This originates from the relative rotation between the beam and column axes ( $\theta_b, \theta_c$ ), as shown in Equation 12.

$$\varphi = \theta_b - \theta_c \quad (\text{Equation 12})$$

Multiplying the load  $P$  with the distance of the column face produced the bending moment, as shown in Equation 13.

$$M = P \times L_{load} \quad (\text{Equation 13})$$

According to Equation 14 and Figure 15 the rotation of the joint is equal to sum of the connection rotational deformation ( $\varphi$ ) and shear deformation of the column web panel zone ( $\gamma$ ).

$$\Phi = \varphi + \gamma \quad (\text{Equation 14})$$

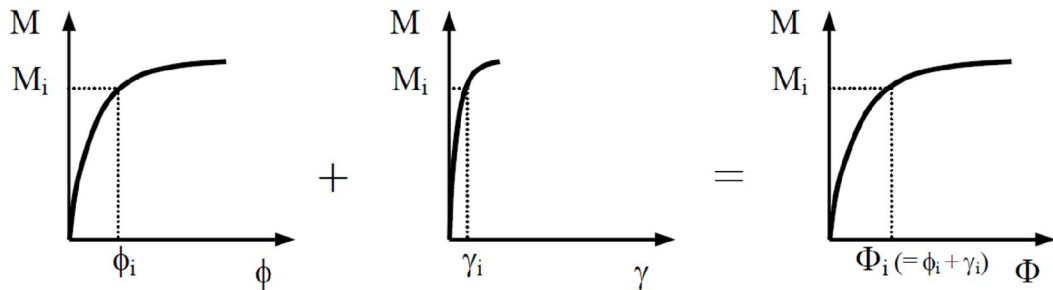


Figure 15: Moment-Rotation Curve of a Joint

The deformability of the connection is due to the couple forces  $F_b$  that appear in flanges of the beam that these forces are statically equal to the bending moment,  $M$ . Figure 16 is the lever arm.

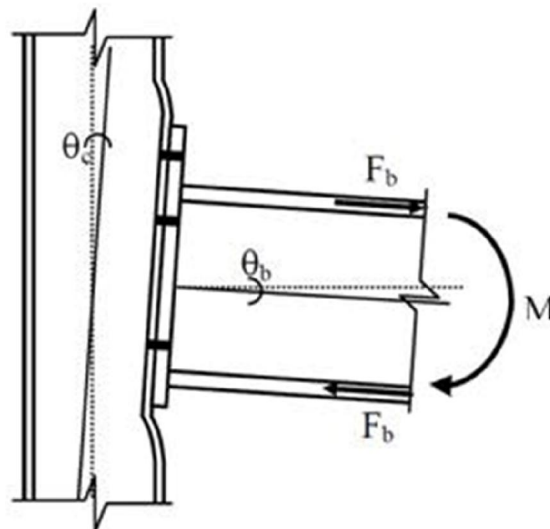


Figure 16: The Rotation of the Beam and Column under the Couple Forces  $F_b$

The two reference points for beam ( $B_1$ ,  $B_2$ ) and two reference points for column ( $C_1$ ,  $C_2$ ) are defined as shown in Figure 17 and displacement values are used to calculate the rotational behaviour of the connection Díaz et al. (2011). The following Figure 18 shows the position of the reference points in 3D model.

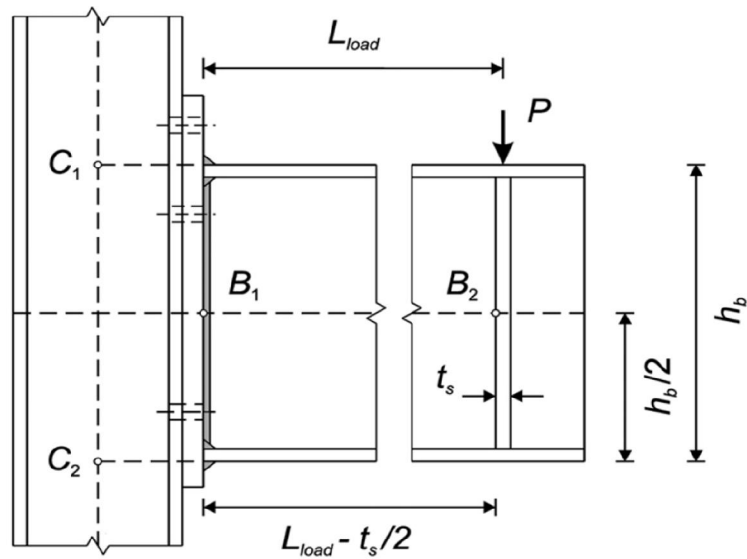


Figure 17: Locations of the Reference Points for Beam and Column  
(Source: Díaz et al., 2011)

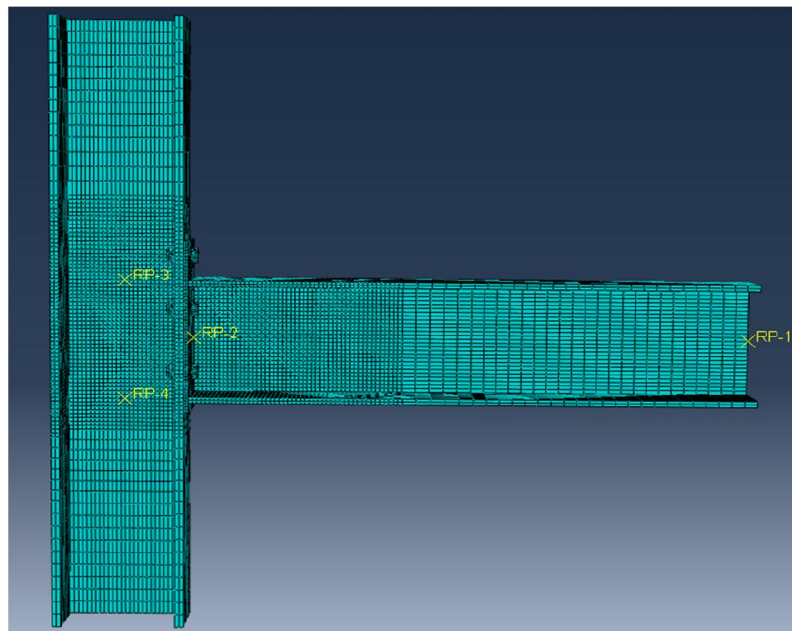


Figure 18: Position of the Reference Points to Determine the Displacement of the Beam and Column

The geometry of the joint is depicted in Figure 19, for the extended end-plate configurations.

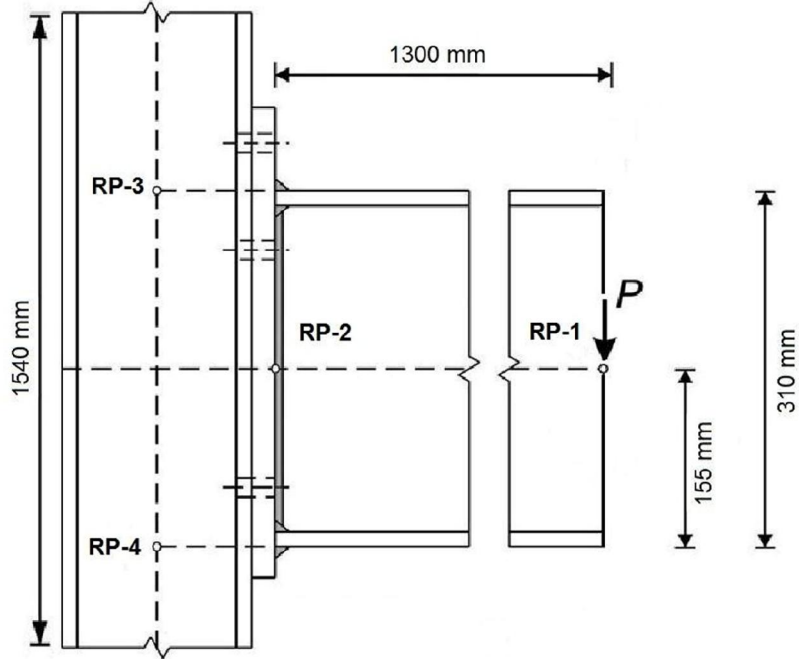


Figure 19: The Geometry of the Joint

Equation 15 is the equation to calculate the rotational deformation of the joint and for the shear deformation of the column web panel Equation 16 was used, and for the connection rotational deformation used Equation 17.

$$\varphi_j = a \tan\left(\frac{V_{B_2} - V_{B_1}}{d_B}\right) - \theta_{el,c} - \theta_{el,b} \quad (\text{Equation 15})$$

$$\gamma = a \tan\left(\frac{U_{C_2} - U_{C_1}}{h_b}\right) - \theta_{el,c} \quad (\text{Equation 16})$$

$$\theta_C = \varphi_j - \gamma = a \tan\left(\frac{V_{B_2} - V_{B_1}}{d_B}\right) - a \tan\left(\frac{U_{C_2} - U_{C_1}}{d_c}\right) - \theta_{el,b} \quad (\text{Equation 17})$$

$V_{B_1}$ ,  $V_{B_2}$  : vertical displacements at points B<sub>1</sub> and B<sub>2</sub>.

$d_B$  :  $L_{load} - T_s / 2$  that is equal to the distance between points  $B_1$  and  $B_2$ .

$\theta_{el,c}$  : The theoretical elastic rotation of column is given by Equation 18.

$$\theta_{el,c} = \frac{5M_j(H - h_c)}{64EI_c} \quad (\text{Equation 18})$$

$\theta_{el,b}$  : The elastic rotation of the beam is given by Equation 19.

$$\theta_{el,b} = -\frac{P}{EI_b} \left( \frac{d_B^2}{6} - \frac{L_{load}d_B}{2} \right) \quad (\text{Equation 19})$$

$I_c$  : The Second moment of areas of the column.

$I_b$  : The Second moment of areas of the beam.

$U_{c1}, U_{c2}$  : The horizontal displacement at the points  $C_1$  and  $C_2$  .

$h_b$  : The distance between points  $C_1$  and  $C_2$  that is equal to the beam height.

## Chapter 4

### EXPERIMENTAL AND FINITE ELEMENT STUDY

#### 4.1 Introduction

The moment-rotation curve can be clarified by experimental testing or finite element simulation based on geometrical properties of the joint. The most reliable way to describe the rotational behaviour of the joint is full scale experimental testing, but performing number of experiments is expensive and time consuming. However, this problem is simplified with the use of finite element analysis program. In this research considered a case study on extended end-plate connection and simulation of the connection is calibrated with the experimental test results. It is possible to decrease the number of expensive experiments by using the calibrated finite element model.

#### 4.2 Experimental Tests

The experimental tests were carried out at the Delft University's structural steel laboratory in Netherland. Two tests were used in this research to verify the finite element part of this study. All the columns and beams used for the investigation are grade S355 (Girao Coelho & Bijlaard, 2007). The details of the specimens and geometry of the end-plate connection are shown in Table 1 and Figure 20, respectively.

Table 1: Details of the specimens (Girao Coelho & Bijlaard, 2007)

NO.	ID	Column		Beam		End-plate		Bolt	
		Section	Grade	Section	Grade	$t_p$	Grade	$\varnothing_b$ (mm)	Grade
1	P10-S690-B8.8	HE300M	S355	HE320A	S355	10.1	S690	24	8.8
2	P15-S690-B12.9	HE300M	S355	HE320A	S355	14.62	S690	24	12.9

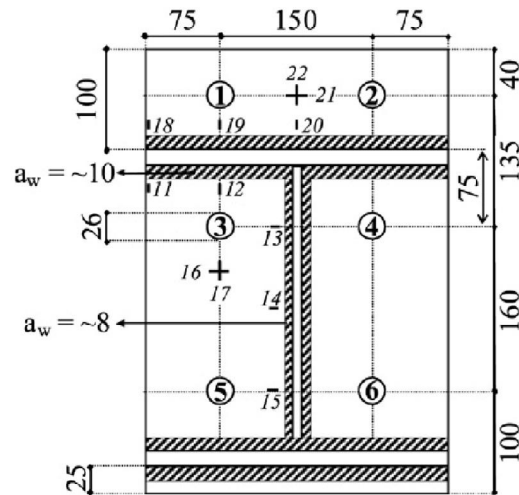


Figure 20: Geometry of the Extended End-Plate Connection  
(Source: Girao Coelho & Bijlaard, 2007)

The specimen was tested under monotonic load that was applied by a 400 kN hydraulic jack and the maximum piston stroke was  $\pm 200$  mm. The loading was carried out under displacement control loading up to failure of the specimen (Girao Coelho & Bijlaard, 2007). The test setup that is used in this experiment is shown in (Figure 21).

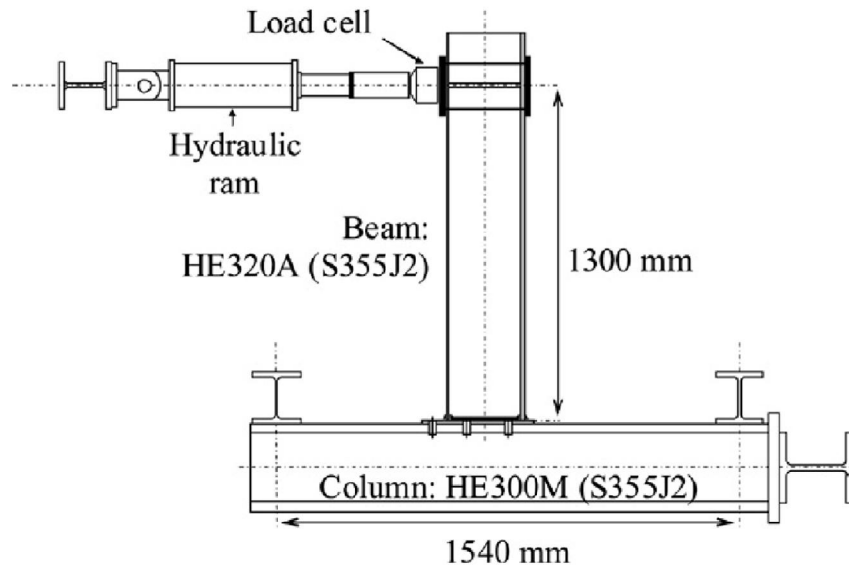


Figure 21: Test Setup in Experimental Test  
 (Source: Girao Coelho & Bijlaard, 2007)

In experimental tests to prevent local deformation under concentrate load a plate with 10 mm thickness was welded to the web and flange of the beam in loading zone, as it shown in Figure 21. The supports were defined in ABAQUS according to experimental test. The supports are depicted in Figure 22.



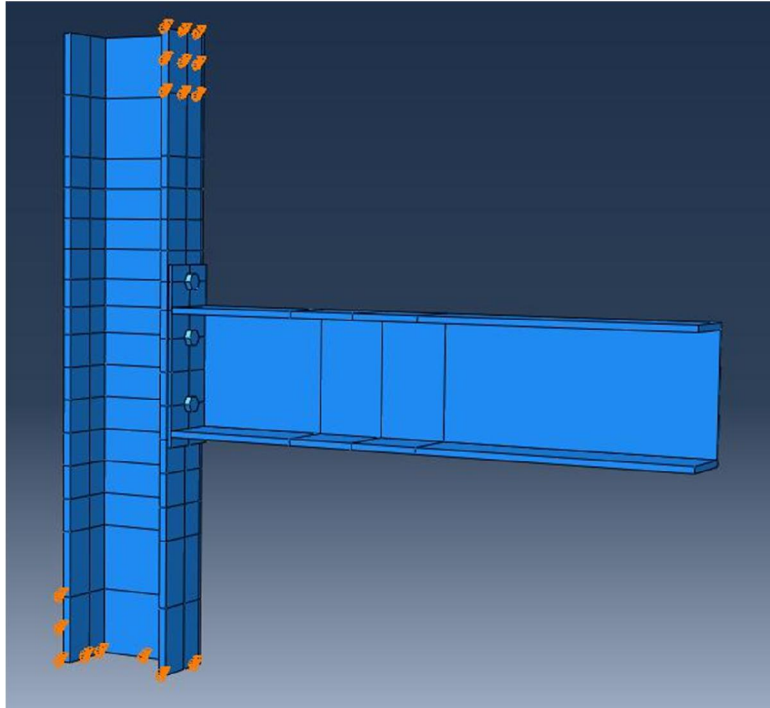


Figure 22: The Supports in 3D Simulation

### 4.3 Details of Finite Element Models

The modeling part of this research included ten extended end-plate connections, as it is shown in Table 2. The parameters investigated in this research were end-plate and bolt steel grade and thickness of end-plate.

Table 2: Dimensions of the joint

NO.	ID	Column		Beam		End-plate		Bolt	
		Section	Grade	Section	Grade	$t_p$	Grade	$\varnothing_b$ (mm)	Grade
1	P10-S690-B8.8	HE300M	S355	HE320A	S355	10.1	S690	24	8.8
2	P10-S355-B8.8	HE300M	S355	HE320A	S355	10.1	S355	24	8.8
3	P10-S275-B8.8	HE300M	S355	HE320A	S355	10.1	S275	24	8.8
4	P15-S690-B12.9	HE300M	S355	HE320A	S355	14.62	S690	24	12.9
5	P15-S355-B12.9	HE300M	S355	HE320A	S355	14.62	S355	24	12.9
6	P15-S275-B12.9	HE300M	S355	HE320A	S355	14.62	S275	24	12.9
7	P10-S690-B10.9	HE300M	S355	HE320A	S355	10.1	S690	24	10.9
8	P10-S690-B12.9	HE300M	S355	HE320A	S355	10.1	S690	24	12.9
9	P15-S690-B8.8	HE300M	S355	HE320A	S355	14.62	S690	24	8.8
10	P15-S690-B10.9	HE300M	S355	HE320A	S355	14.62	S690	24	10.9

#### 4.4 Finite Element Modeling

Finite Element Method (FEM) is one of the most suitable and useful tool for analysis, design and modeling. Preparing experiment is expensive and time consuming. Experiments are a necessary part of research and finite element can reduce the cost of research. Earlier in finite element simulations models were highly simplified, today by using powerful computers engineers are able to model more complicated structures easily but it this does not mean that the connection

simulations are close to the real.

The important curve that shows the behaviour of the connection is moment- rotation curve which represent the ductility of the connection. This curve depends on some parameters such as:

- Geometrical and material of the element and plastic behaviour of the materials
- Pretension force of the bolts
- Contacts between bolt head and plate, bolt shank and nut, bolt shank and column, bolt shank and holes and between nut and column and the interaction between plate and column face
- Welds

If all the parameters considered in the modeling, again there will be some approximations that have great effect on the analysis. These approximations are:

- The finite element program
- Element type
- Meshing of the component
- Number of the finite elements used
- Boundary conditions
- Rate of loading
- Temperature

In spite of these simplifications the result of finite element method is highly accurate. The simulation takes considerable amount of time depending on the computational power of the personal computers.

The finite element analysis carried out using the ABAQUS (version 6.11) software. This finite element package has the capability to model complex steel connection with accurate detail such as contact problem, non-linear material and etc.

The end-plate connection test setup includes column, beam, plate, bolts and nuts. For the contact surface special attention was given to the modeling. For instance, contact between plate, column face and bolts were attended.

#### **4.4.1 Symmetric Modeling**

The geometry of the end-plate connection is symmetrical through the beam web, for this reason only half of the connection was modeled. For the surface on the symmetry line a boundary condition was defined and the perpendicular displacement and rotation on that face took in to account zero but tangential rotation and displacement allowed to exist. Figure 23 is shown a symmetrical model of end-plate connection.

Symmetric modeling is a technique to reduce the cost of analysis by just considering half of the model. When one model is symmetric then that loading and geometry will be symmetrical too. All the nodes on the plane of symmetry are restrained for translation in symmetric direction. In this research for extended end-plate connection only half of the model in considered and modeled as a symmetric model (Figure 23) for achieving the simplicity and reducing the time required for analysis.

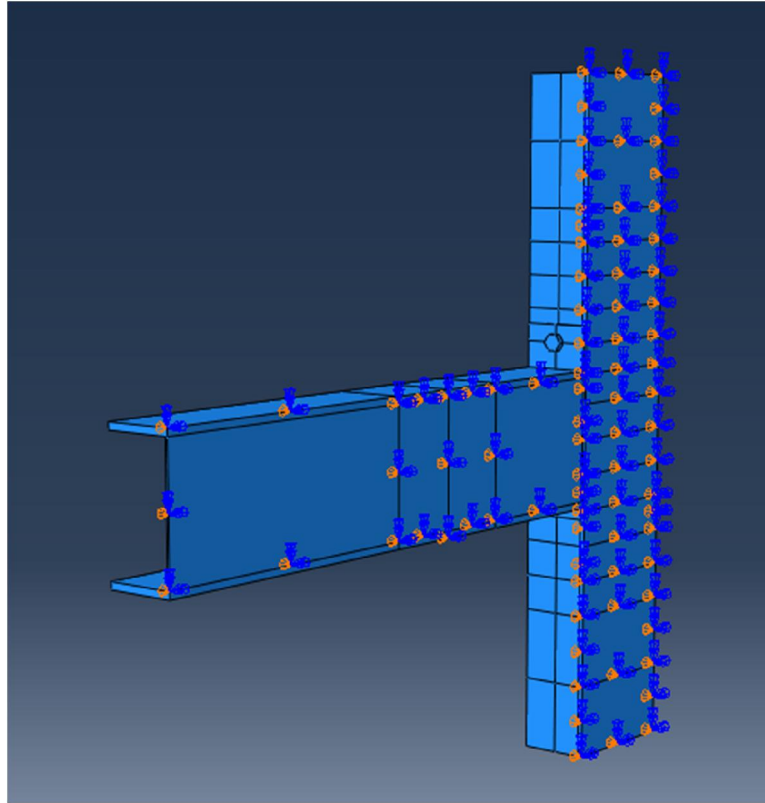


Figure 23: Symmetric Modeling of an End-Plate Connection

#### 4.4.2 Material

The material definition is an important part of finite element analysis, and each component should be defined carefully and all parts should be defined with appropriate material parameters. The temperature is not considered in this research.

Materials initially have elastic behaviour which means material deforms under load and after the removal of the applied load it can fully recover to original shape, when the load is increased more than the yielding point, then the material do not return to original shape.

In ABAQUS software true stress and true strain used to define the non-linear behaviour of material properties. The data from tensile testing represent nominal

stresses and strains and they should be converted to true stresses and strains. The Equation 20 is used to convert nominal strain to true strain.

$$\varepsilon_{true} = \ln(1 + \varepsilon_{nom}) \quad (\text{Equation 20})$$

where

$\varepsilon_{true}$  is the true strain

$\varepsilon_{nom}$  is the nominal strain

The true stress is a function of the nominal strain and nominal stress, as it is seen in the Equation 21.

$$\sigma_{true} = \sigma_{nom} (1 + \varepsilon_{nom}) \quad (\text{Equation 21})$$

The total true strain value can be divided into the elastic true strain ( $\varepsilon_{el, true}$ ) and plastic true strain ( $\varepsilon_{pl, true}$ ). The true elastic strain is equal to the true stress divided by the Young's modulus (E). For the explicit analysis the true plastic strain is required and it can be obtained from Equation 22.

$$\varepsilon_{pl, true} = \varepsilon_{true} - \varepsilon_{el, true} = \ln(1 + \varepsilon_{nom}) - \frac{\sigma_{true}}{E} \quad (\text{Equation 22})$$

The materials were defined in terms of stress-strain curve and assigned to components. A steel grade of S355 is used for the beam and column and steel grades of S275, S355 and S690 are used for the end-plate respectively. Steel grades of 8.8, 10.9 and 12.9 are used for bolts and nuts. Von Mises yield criteria was used for all material.

Mechanical properties for the structural steels that are used in these simulations are given in Table 3.

Table 3: Mechanical properties of the structural steel

Material type	Yield stress (N/mm <sup>2</sup> )	Ultimate stress (N/mm <sup>2</sup> )	Density (Kg/m <sup>3</sup> )	Young's modulus (KN/mm <sup>2</sup> )	Poisson ratio
S275	275	450	7850	205	0.3
S355	355	550	7850	205	0.3
S690	690	823	7850	205	0.3
8.8 Bolt	640	800	7850	205	0.3
10.9 Bolt	900	1031	7850	205	0.3
12.9 Bolt	1080	1200	7850	205	0.3

The linear elastic behaviour of materials was defined within the material definition while defining the elasticity in ABAQUS (ABAQUS inc, 2006). In the elastic plastic analysis ABAQUS assumed the deformation being caused by the plastic strain because the elastic strains are small. In ABAQUS, the plasticity theory was used for non-recoverable deformation response.

In incremental theories the mechanical strain rate is divided to two parts, elastic part and plastic part.

#### 4.4.3 Bolt Pretension

The first step in loading in this model is bolt pretension. In these simulations different components (bolt head, bolt shank and nut) was modeled with three-dimensional solid elements. The interactions between surfaces of the bolt were defined and for effect of tightening of the bolt, the pretension force of the bolt was applied in ABAQUS.

The pretension force of the bolt was applied according to AISC (2005). AISC (2005) defined pretension load as 70% of the bolt's ultimate tensile strength.

The pretension load was applied on an arbitrary plane that created on the bolt shank and the direction of the load was perpendicular to the longitudinal axis. In this research, these values are used in the simulations to account for tightening of bolts. The bolt pre-load applied is given in Equation 23.

$$F_p = 0.7f_{y,b} \times A_s \quad \text{(Equation 23)}$$

#### **4.4.4 Interface Modeling**

Two algorithms (surface-to-surface and node-to-surface) used in ABAQUS are deformable finite element. Friction is an important factor in contact algorithm.

The contact surface between bolt shank and nut, bolt shank and end-plate, bolt head and end-plate, bolt shank and column, nut and column was defined by nonlinear algorithm due to difference in friction between surfaces. All the surfaces are defined in terms of pairs, and the larger part defined as a master surface and smaller part defined as slave surface. The surfaces were defined in surface-to-surface and node to surface properties, and for two surfaces it is not possible to use the same algorithms. Tie algorithm was used to simulate the behaviour of welding part of the connection. Tie algorithm was simulated the behaviour of welding part by preventing the friction between two components, as shown in Figure 24.



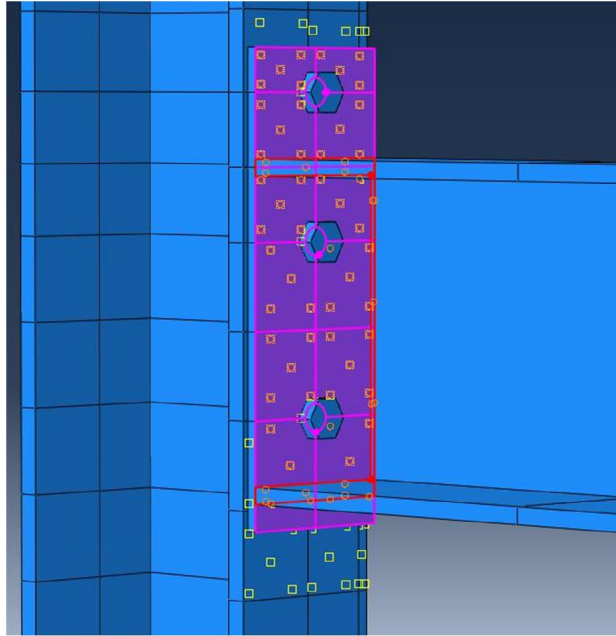


Figure 24: The Contact between Beam and Plate

#### 4.4.5 Consideration of Friction

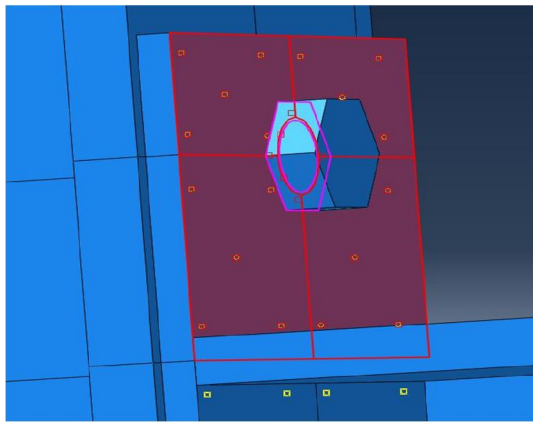
One of the important factors on slipping of two components and moment- rotation curve that shows the behaviour of the connection is friction value. In previous research that was based on experimental study, they did not mention about the effect of friction from the main components, Kukreti and Abolmaali (1999). In their tests they did not suggest anything about the friction between surfaces.

In AISC (2005), there are two classes to define the friction coefficient between surfaces:

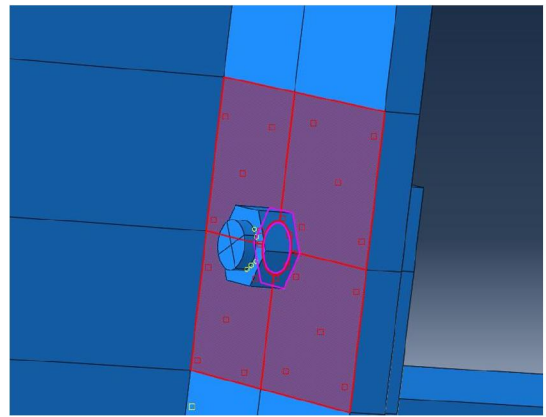
- Class A: in this class surfaces are unpainted, mill scale or surfaces with Class A coatings on blast-cleaned steel surfaces. The mean friction coefficient ( $\mu$ ) is equal to 0.35.
- Class B: in this class surfaces are unpainted blast-cleaned steel. The mean friction coefficient ( $\mu$ ) is equal to 0.5.

The mean friction coefficients depend on the condition of the surfaces in the connection, and it will be different from one test to another one.

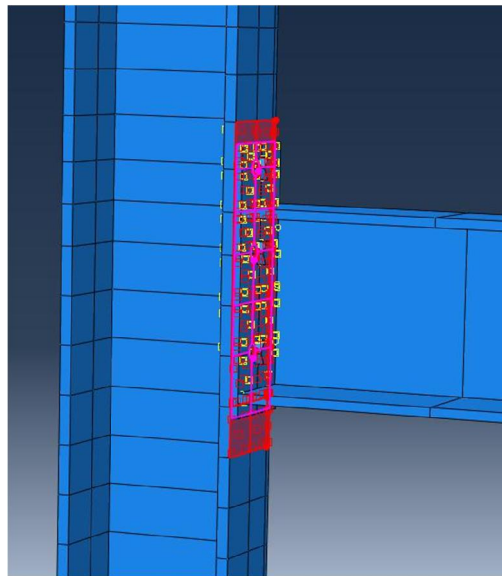
In this simulation Class A surfaces is used to define the interaction between end-plate and column face, bolt head to the plate and nut to the column (Figure 25). The friction coefficient was 0.35.



(a) Interaction between Bolt Head and Column



(b) Interaction between Nut and Column



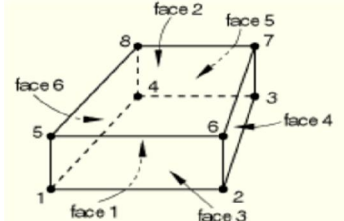
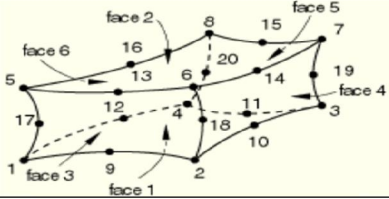
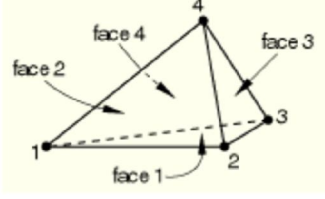
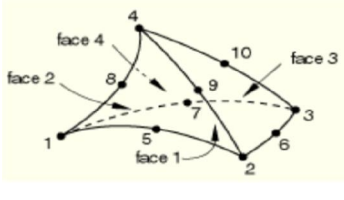
(C) Surface Contact between Plate and Column

Figure 25: Contact between Different Components of the Connection

#### 4.4.6 Meshing

ABAQUS software contains a large variety of elements, but in finite element analysis the current ABAQUS library suggests a number of hexahedron elements. All the connection components were modeled using the element C3D8R that is three dimensional 8-noded brick element (Table 4). The element has three degrees of freedom in x, y and z direction.

Table 4: Various elements used in ABAQUS (ABAQUS inc, 2006)

Element	Description	D.O.F.	Element shape
C3D8R	Hexagonal Element	24	
C3D20R	Hexagonal Element	60	
C3D4	Tetrahedral Element	12	
C3D10M	Tetrahedral Element	30	

Since the components have plastic deformation then the stress will distribute and distribution of contact stress is very important in the simulation. For this reason the model should have enough mesh density (ABAQUS inc, 2006). The critical zone is

near the connection. As it is shown in Figure 26 the mesh density increased in critical zones. It goes to reduce the analysis cost in this simulation.

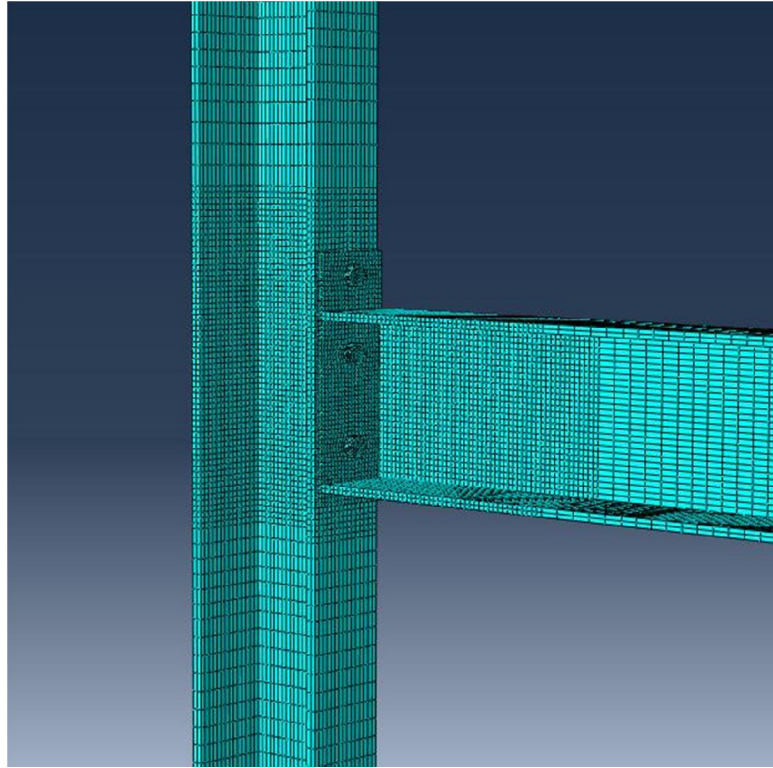


Figure 26: Detail of the Mesh Model of the Joint

#### 4.4.7 Coupling

To prevent the local deformation of the beam under concentrated force, the end of the beam cross section was defined as a coupling point in ABAQUS (Figure 27). For this reason  $d_B$  is equal to  $L_{load}$  for the Equations from 15 to 19.

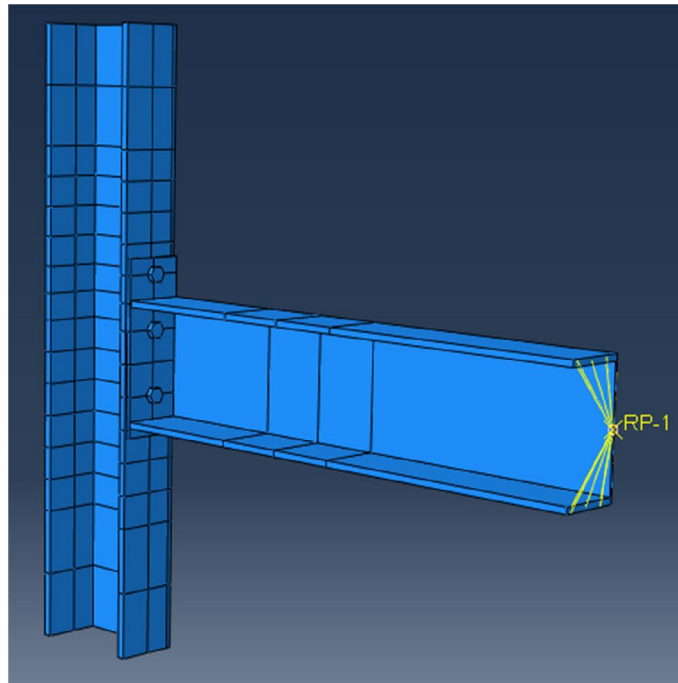


Figure 27: Coupling Point for Reference-Point 1

#### 4.4.8 Dynamic Analysis

In ABAQUS, there are two different categories for dynamic analysis, in these types of analysis two different strategies are used as given below:

##### 4.4.8.1 Implicit

The implicit analysis is based on static equilibrium, and the important feature of the implicit solution procedure is global stiffness matrix. And this type of analysis characterized by the assembly of a global stiffness matrix and simultaneous solution of a set of linear or nonlinear equations (Van Der Vegte, 2004). With this method wide range of linear and nonlinear analysis can be obtained. Newton-Raphson is used for most nonlinear analyses to converge the solution along the force deflection curve in each step, but Newton-Raphson method is unable to achieve the convergence if the tangent stiffness is equal to zero. For solving this problem, Arc-Length algorithm (Riks method) is used to make it possible that load and displacement vary throughout the time step (ABAQUS inc, 2006).

#### 4.4.8.2 Explicit

In the explicit method, at the end of an increment (time  $t + \Delta t$ ) the state of the model is only based on displacements, velocities and accelerations, and for each nodes these data will record. The nodal velocities at time  $t + \Delta t$  is calculated by assuming that the acceleration is constant during a time in an increment  $\Delta t$ . For displacement calculation of one node, at the end of the increment displacement can be calculated by adding the displacements during the time increment  $\Delta t$  to the displacement at time  $t$  (van der Vegte, 2004). For complicated contact simulations explicit analysis is much easier than implicit analysis, this is one of the important advantages of explicit analysis to implicit one (ABAQUS inc, 2006).

A comparison between CPU time and model size for both explicit and implicit analysis is shown in Figure 28. It is suitable to use implicit for small models and for large models explicit method may be favorable and needs less system resources than the implicit one. These factors become more valid when disk space and memory of the computers that are used for this research are limited (Van Der Vegte, 2004).

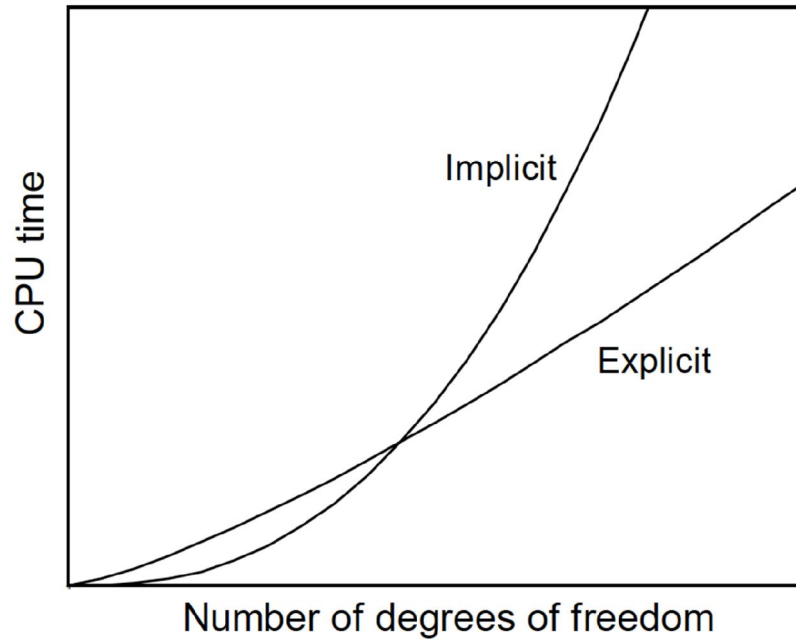


Figure 28: Comparison between Implicit and Explicit

## Chapter 5

### RESULTS AND DISCUSSIONS

#### 5.1 Introduction

This chapter contains the result of the finite element analysis of the high strength extended end-plate connections and compares the result of different analysis to understand the behaviour of the connections under variation of the end-plate thickness and steel grade of the end-plate and bolts.

#### 5.2 Finite Element Results

The deformation of the model is mainly caused by the end-plate deformation and the elongation of the bolts. At the tension beam flange level the deformation of the end-plate is described in terms of the distance between the plate and the column flange. These simulations indicate that the deformation of the end-plate increases when the thickness of the plate decreases. The simulation results can be seen in Table 5. In these models the column had little deformation and behaves approximately like a rigid element. For this reason the shear deformation of the column web panel zone ( $\gamma$ ) and the relative rotation of the column axe  $\theta_c$  are approximately equal to zero and the rotation of the connection is equal to the rotation of the joint.



Table 5: Maximum bending moment and maximum connection rotation results

ID	$M_{max}$ (N – mm)	$\varphi_{Mmax}$ (rad)
P10-S690-B8.8	254946000	0.05684
P10-S355-B8.8	235632000	0.06281
P10-S275-B8.8	224617000	0.06691
P10-S690-B10.9	257562000	0.05517
P10-S690-B12.9	264235000	0.05301
P15-S690-B12.9	366855000	0.01928
P15-S355-B12.9	299162000	0.03150
P15-S275-B12.9	259907000	0.03624
P15-S690-B10.9	365188000	0.02002
P15-S690-B8.8	312000000	0.01575

The following figures illustrate the end-plate at failure conditions for each of the model. Plastic deformation of the end-plate is more evident in the specimens with lower steel grade and plate thickness.

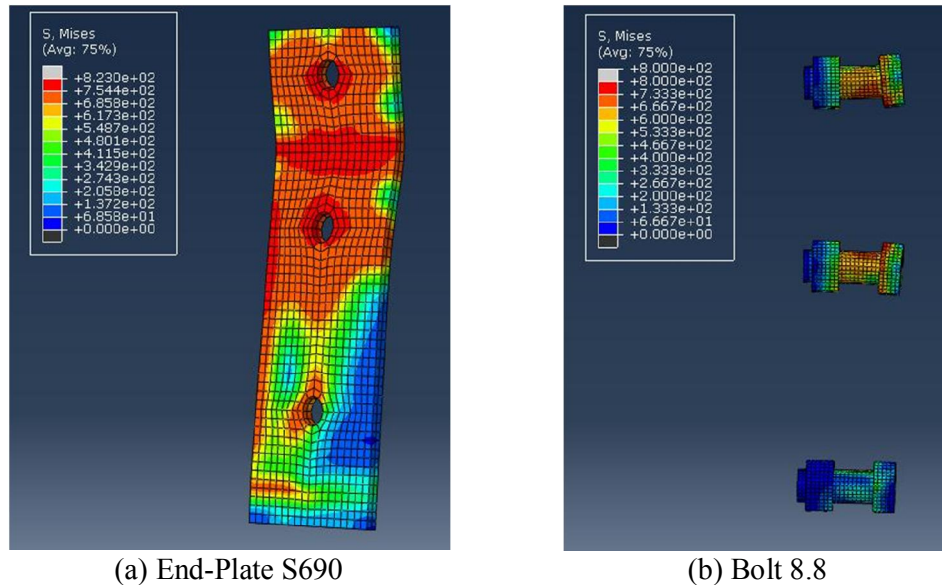


Figure 29: Specimen P10-S690-B8.8

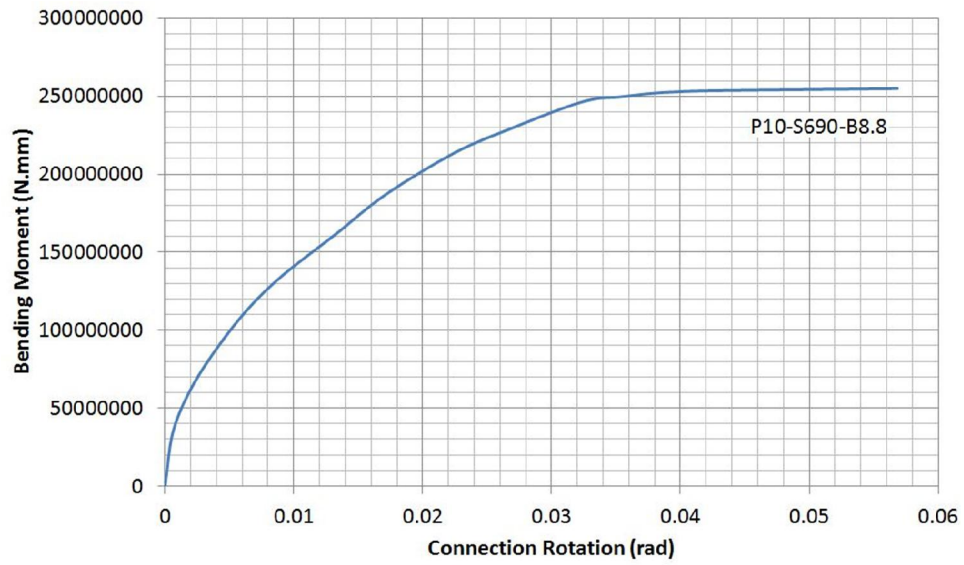


Figure 30: Moment-Rotation Curvature for Specimen P10-S690-B8.8

As it depicted in Figure 29 and Figure 30, failure took place in the end-plate but the bolts were not yielded at that time. But the bolt head had deformation. The mode of failure for this connection is mode I.

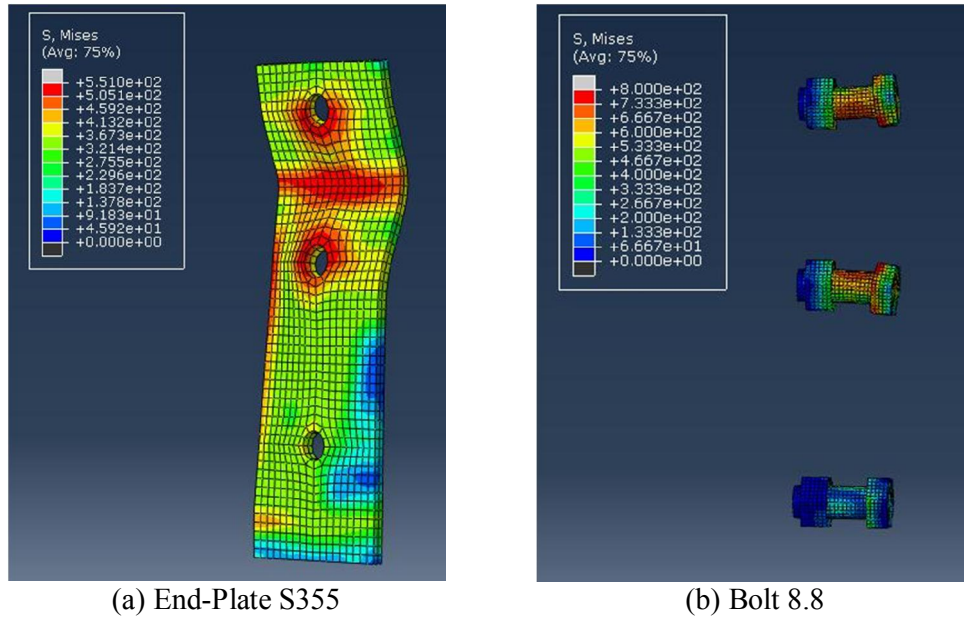


Figure 31: Specimen P10-S355-B8.8

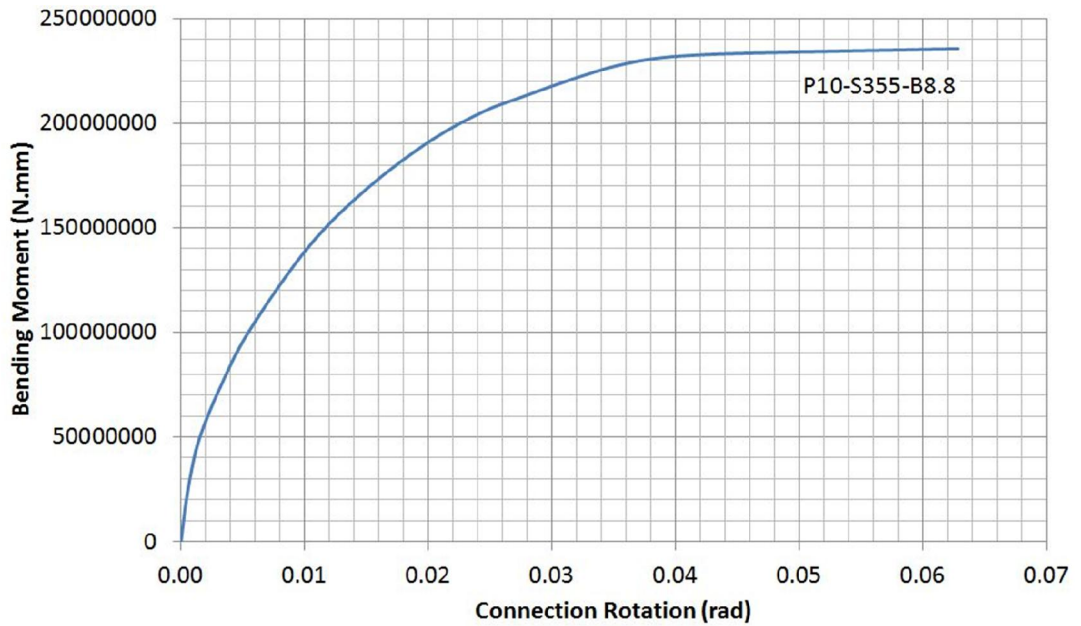


Figure 32: Moment-Rotation Curvature for Specimen P10-S355-B8.8

In the P10-S355-B8.8 the steel grade of the end-plate changed to S355 for evaluating the behaviour of the ductility of the connection. This connection had shown more ductility than the connection with S690 plate but there was reduction in the moment

resistance. The mode of failure was mode I, and the plate was yielded first (Figures 31, 32).

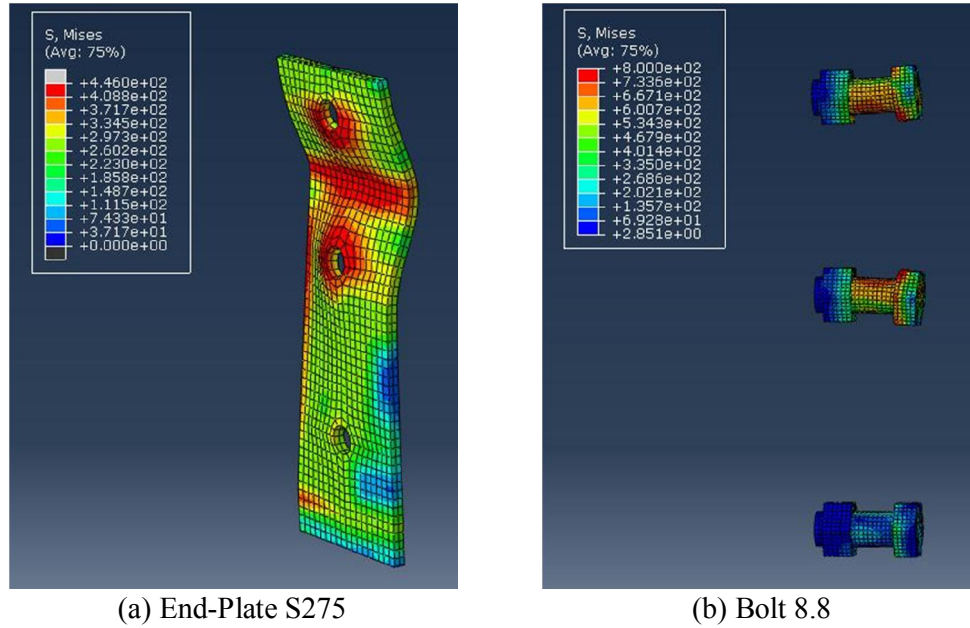


Figure 33: Specimen P10-S275-B8.8

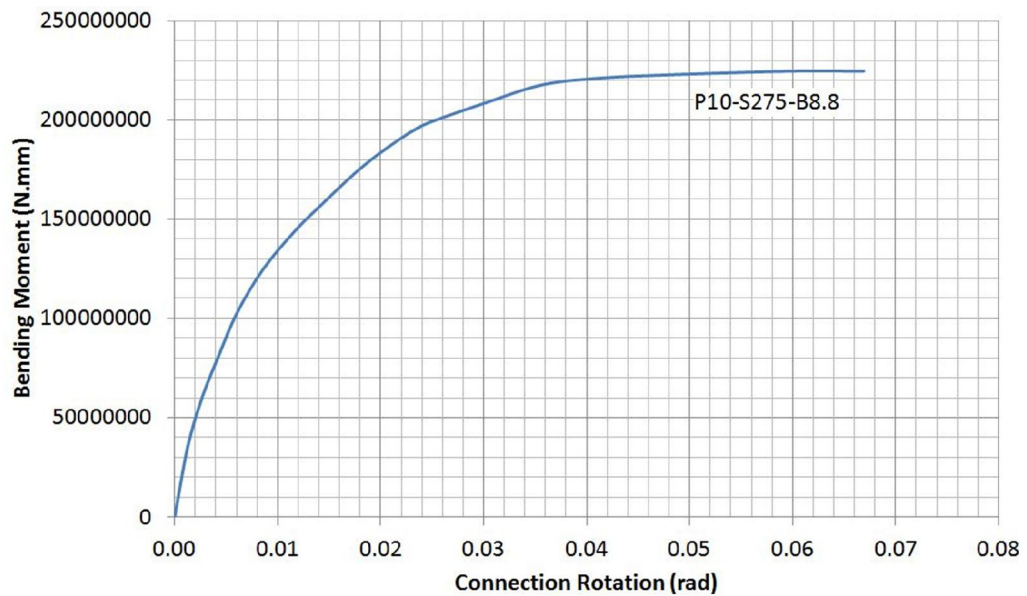


Figure 34: Moment-Rotation Curvature for Specimen P10-S275-B8.8

In the next simulation, the plate steel grade decreased to investigate the behaviour of the connection. The simulation shown the ductility of the connection increased but

the moment resistance decreased. The mode of failure for this connection was mode I according to Eurocode 3. The S275 plate had more deformation than S355 and S690 (Figures 33, 34).

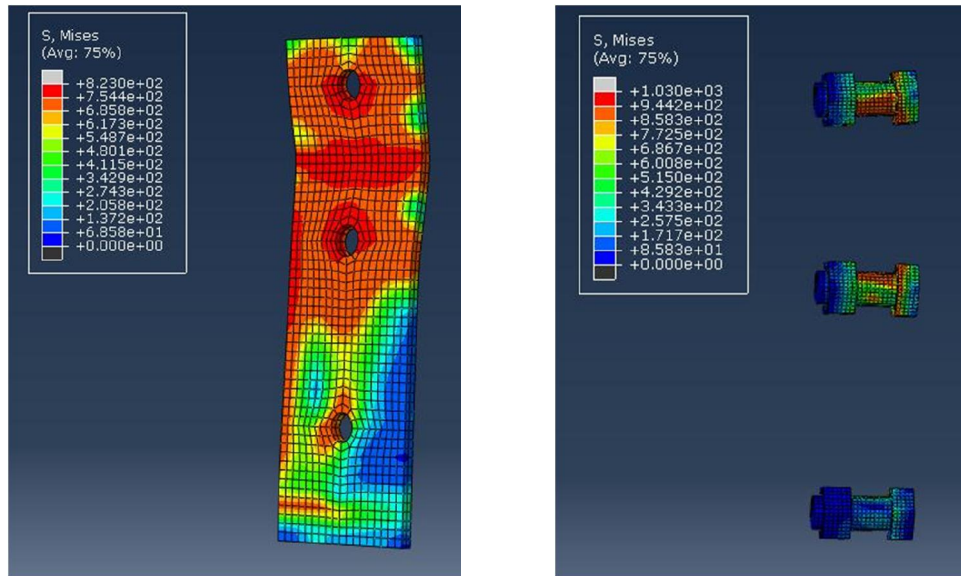


Figure 35: Specimen P10-S690-B10.9

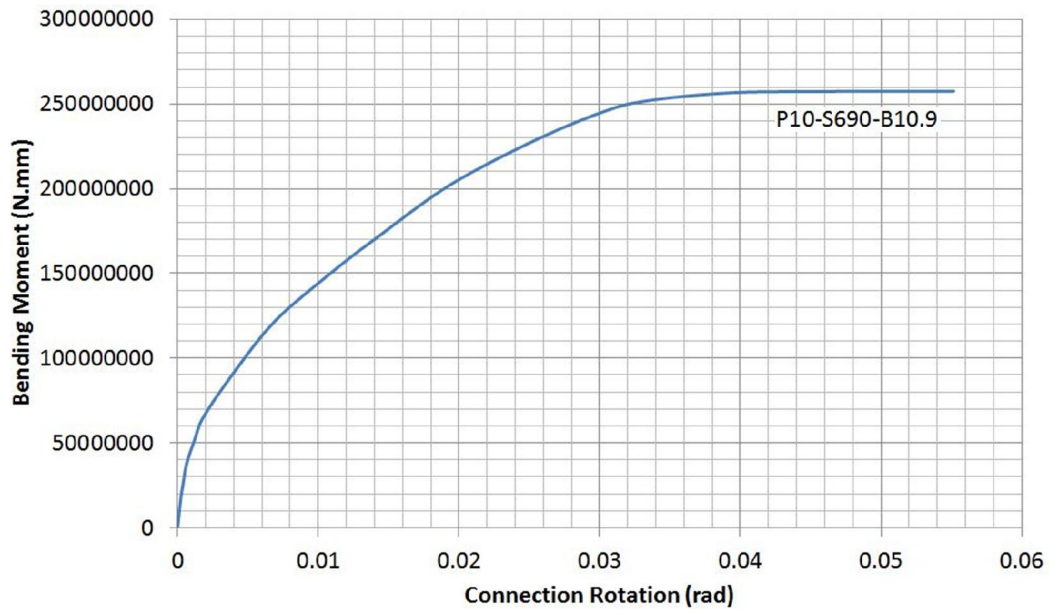


Figure 36: Moment-Rotation Curvature for Specimen P10-S690-B10.9

In this simulation the bolt grade was change to see the effect of increasing the bolt grade on behaviour of the connection. Results show that increasing the bolt grade causes decrease in the ductility of the connection. But it shows little more moment resistance at the same time. In this simulation plate was yield first and the mode of failure is mode I (Figures 35, 36).

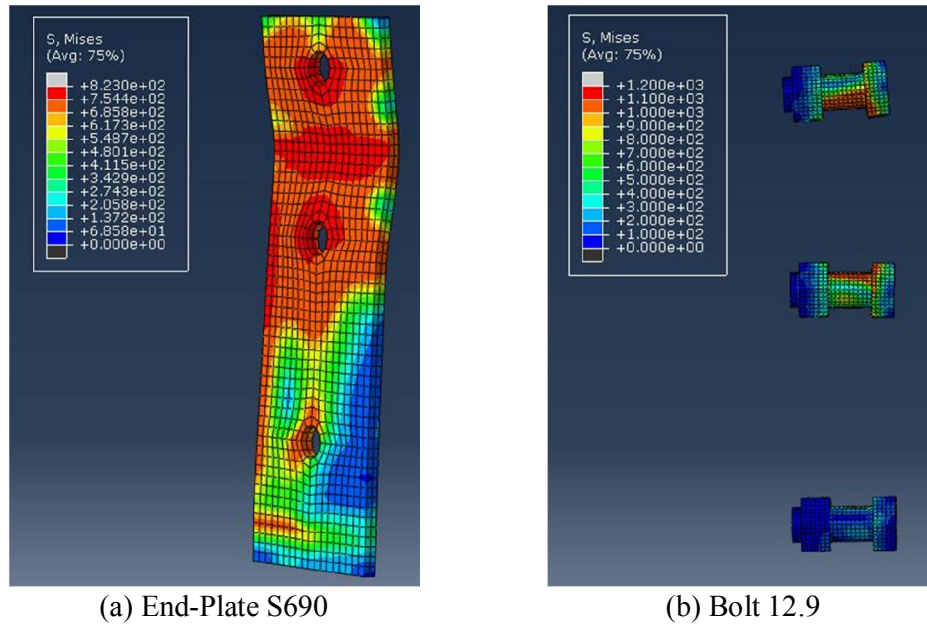


Figure 37: Specimen P10-S690-B12.9

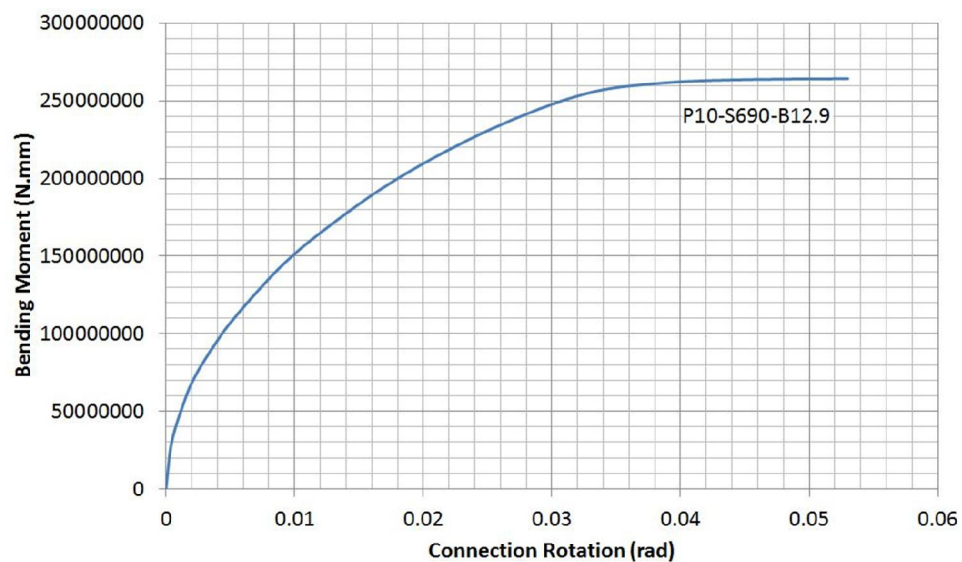
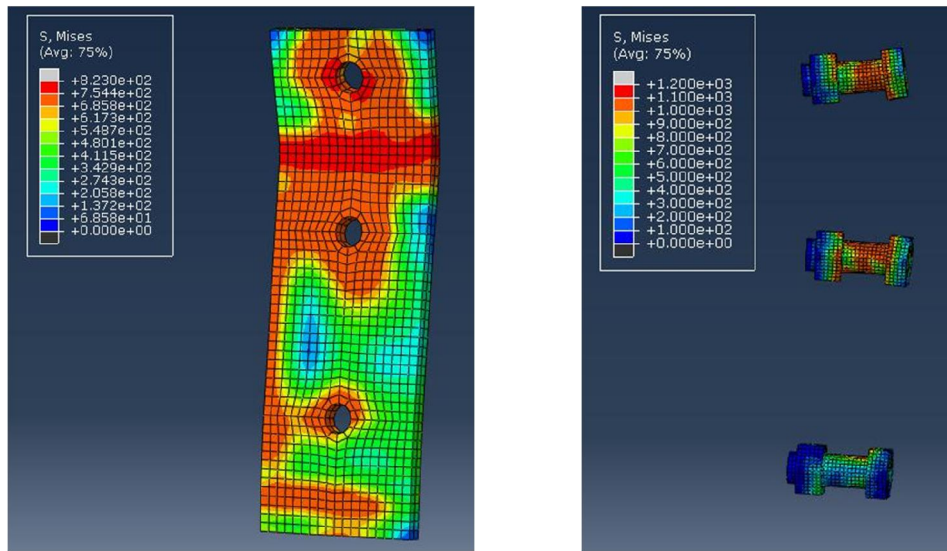


Figure 38: Moment-Rotation Curvature for Specimen P10-S690-B12.9



P10-S690-B12.9 showed stiff behaviour than previous specimens resulted by using the bolt grade higher than other specimens. Ductility decreased and bolts shown little plastic deformation. Mode I is the mode of failure for this connection according to the Eurocode 3 (Figures 37, 38).



(a) End-Plate S690 (b) Bolt 12.9

Figure 39: Specimen P15-S690-B12.9

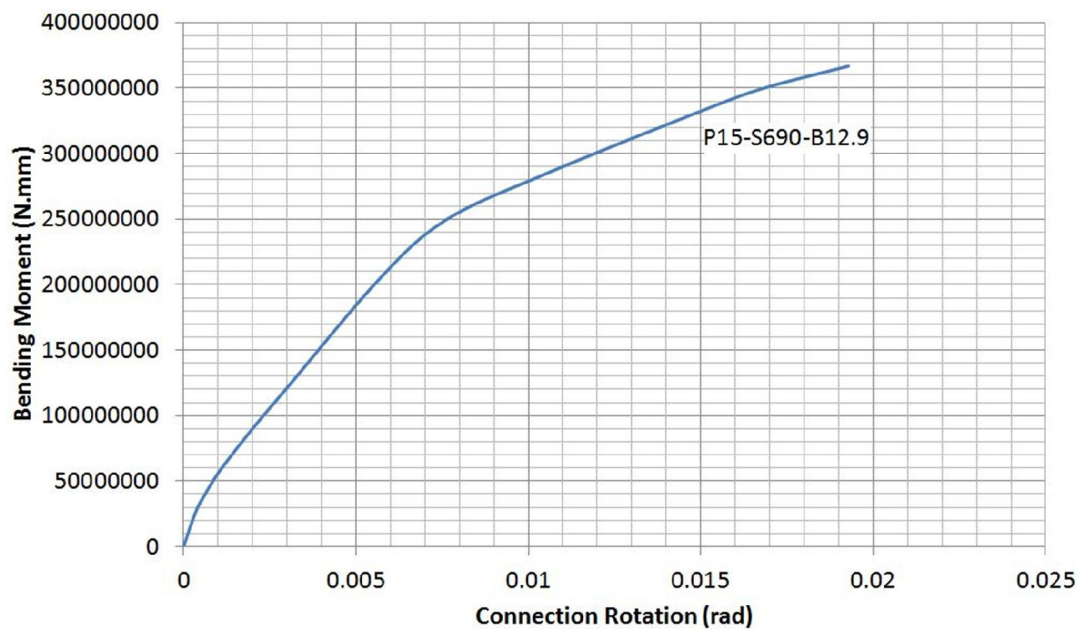


Figure 40: Moment-Rotation Curvature for Specimen P15-S690-B12.9

In this series of connection the end-plate thickness increased to 15 mm. The main idea is the behaviour of the connection with different steel grade for plate in different thickness.

P15-S690-B12.9 shown stiff behaviour than other specimens and the ductility of the connection was lower than other connection but the failure was happened again in the end-plate (mode I) (Figures 39, 40).

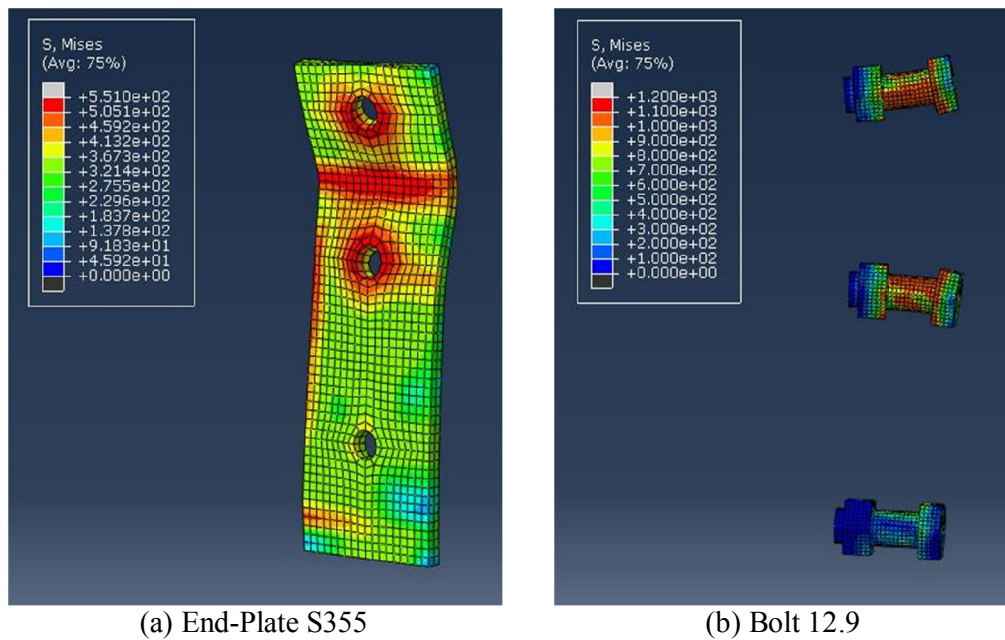


Figure 41: Specimen P15-S355-B12.9



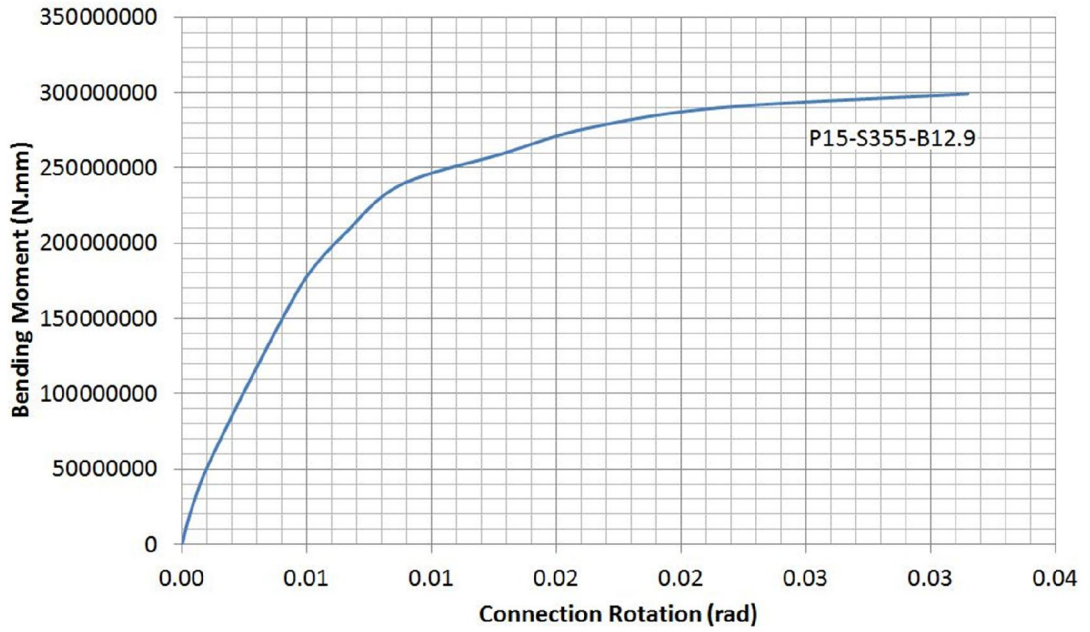
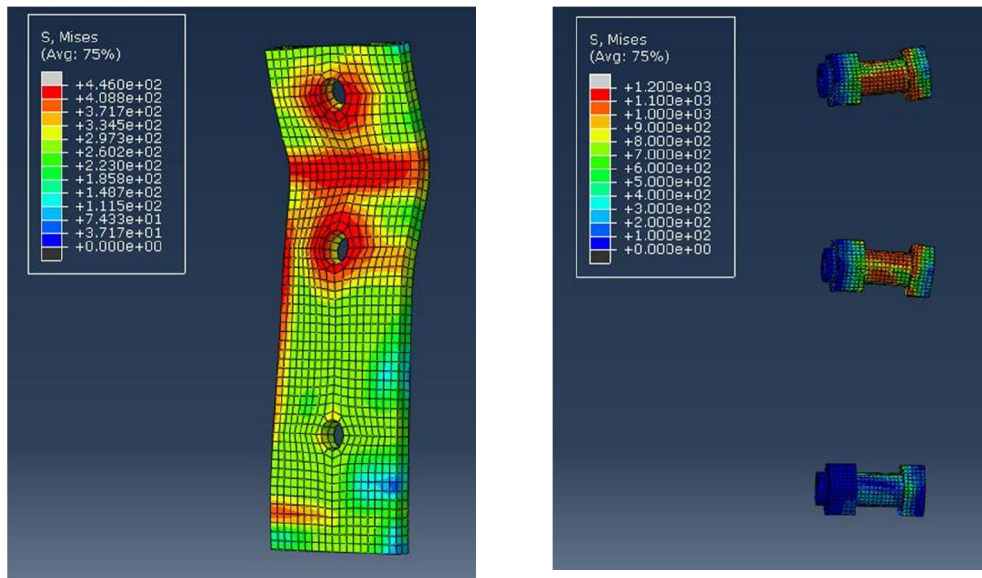


Figure 42: Moment-Rotation Curvature for Specimen P15-S355-B12.9

P15-S355-B12.9 was simulated to investigate the effect of the steel grade on the plate and the connection. As it was expected the plastic deformation of the end-plate and the ductility of the connection increased. But the mode of failure for this connection did not change (Figures 41, 42).



(a) End-Plate S275

(b) Bolt 12.9

Figure 43: Specimen P15-S275-B12.9

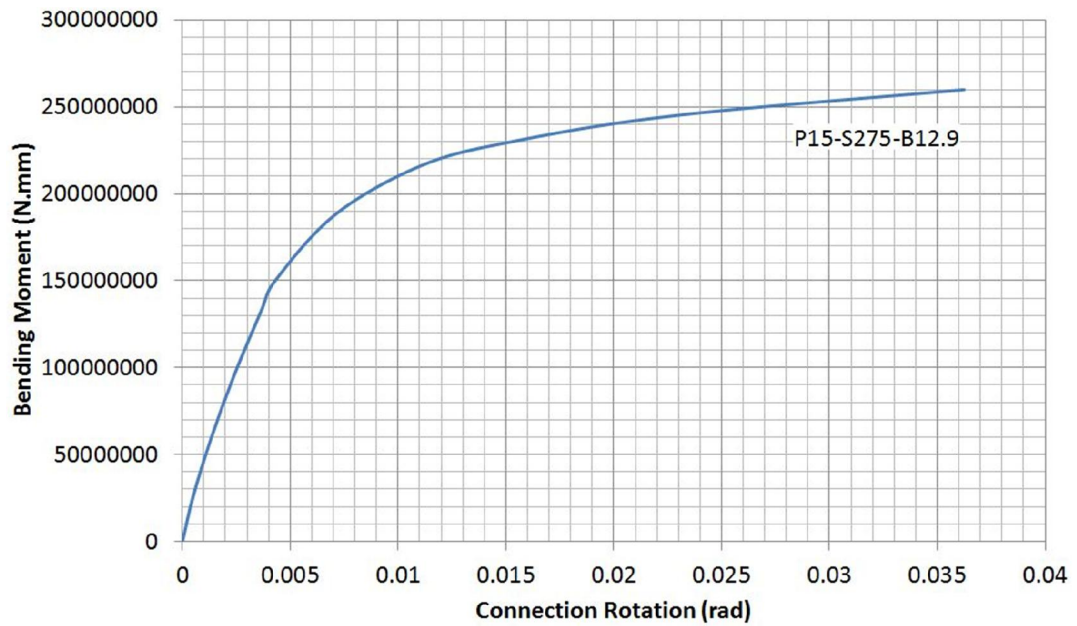
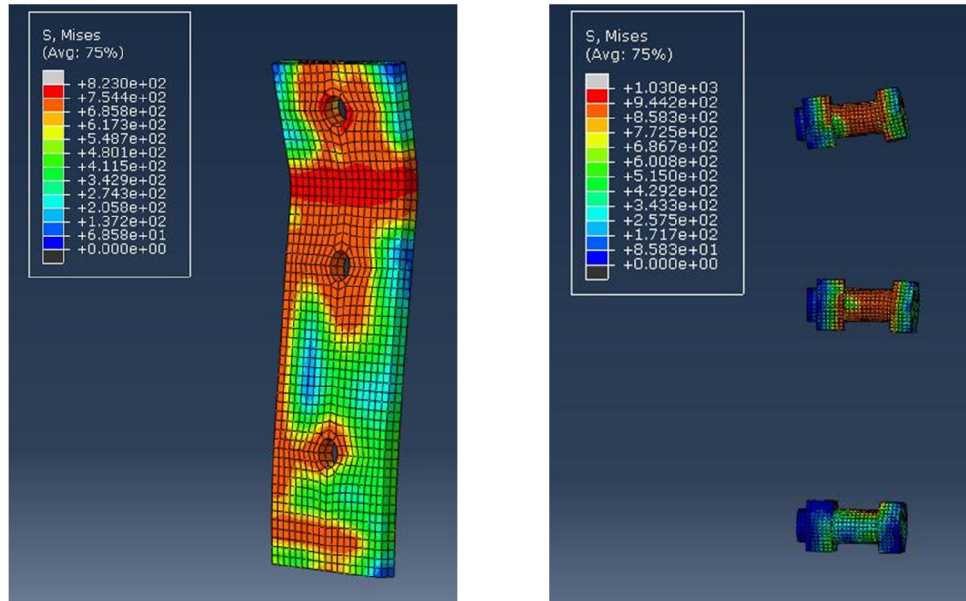


Figure 44: Moment-Rotation Curvature for Specimen P15-S275-B12.9

The P15-S275-B12.9 shown more ductility than P15-S355-b12.9 but the moment resistance was decreased. Because of reduction in strength of the plate, the plate had more deformation, but plate yield at the lower amount of bending moment than the plate with S355 steel grade (Figures 43, 44).



(a) End-Plate S690 (b) Bolt 10.9

Figure 45: Specimen P15-S690-B10.9

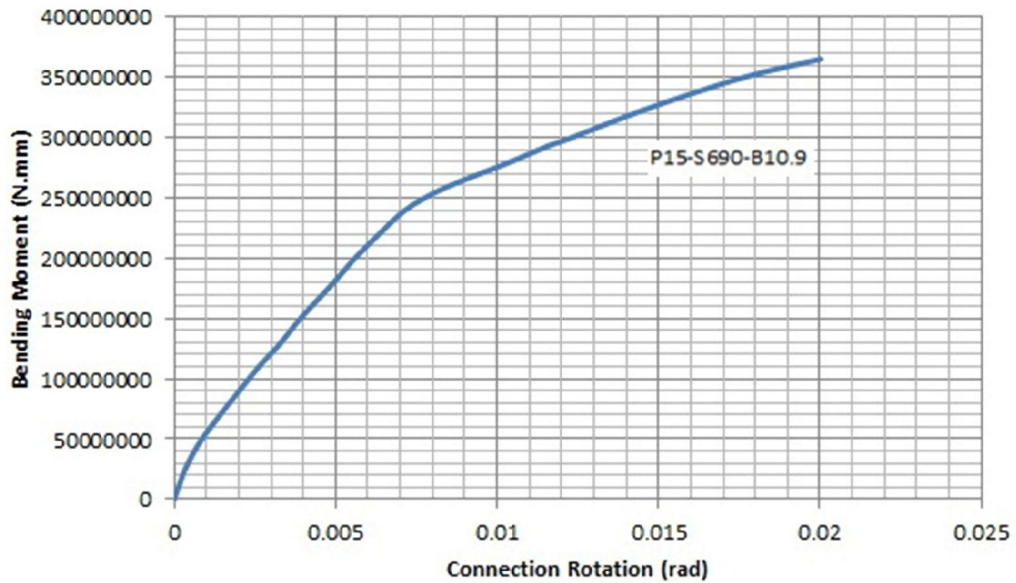
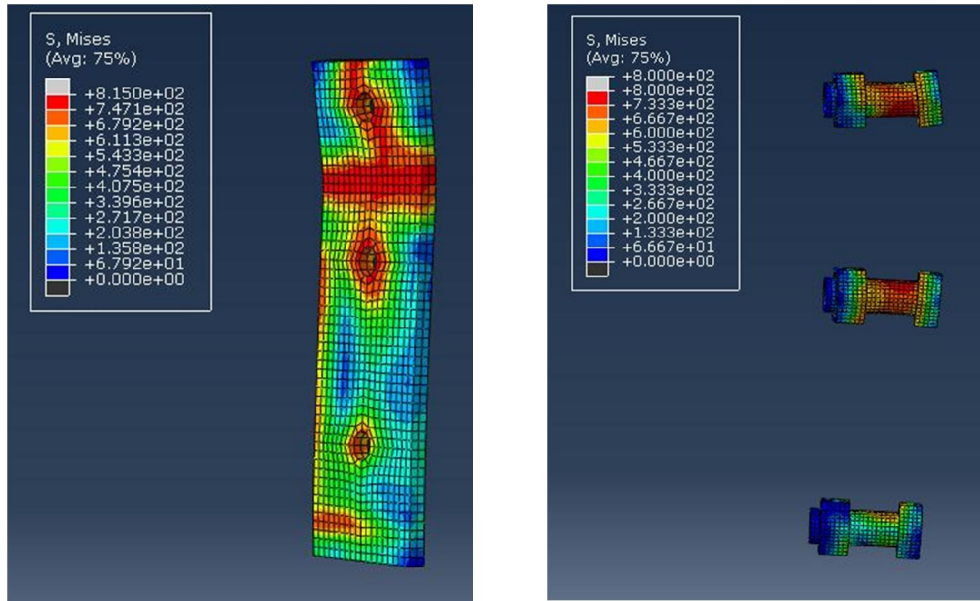


Figure 46: Moment-Rotation Curvature for Specimen P15-S690-B10.9

By decreasing the bolt grade in the specimen P15-S690-B10.9 the ductility of the connection increased. By decreasing the bolt grade the plastic deformability of the bolt will increase (Figures 45, 46).



(a)End-Plate S690 (b) Bolt 8.8

Figure 47: Specimen P15-S690-B8.8

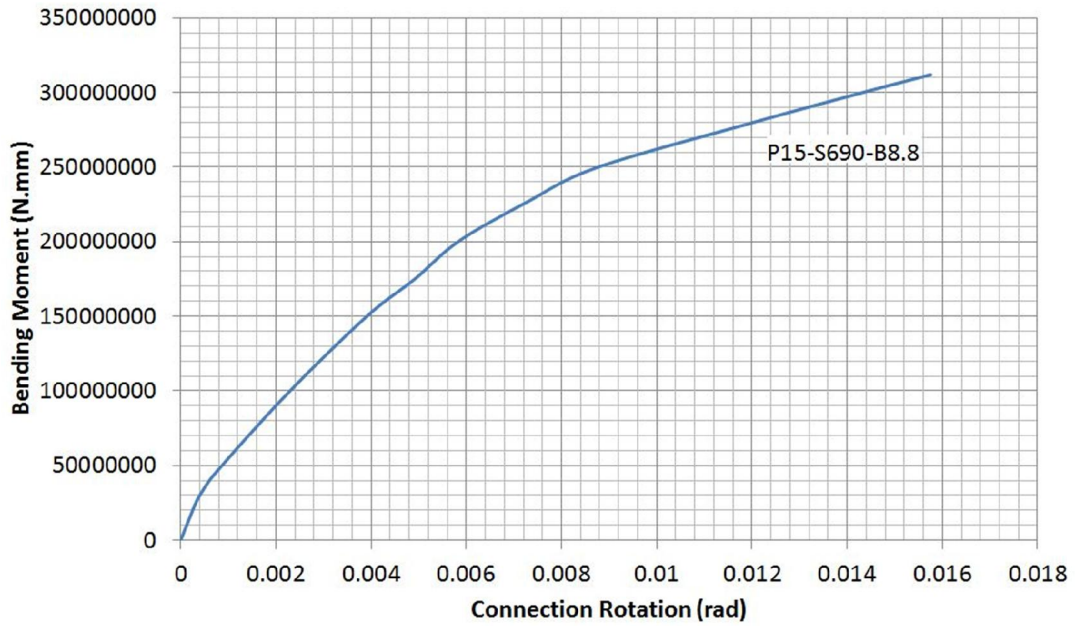


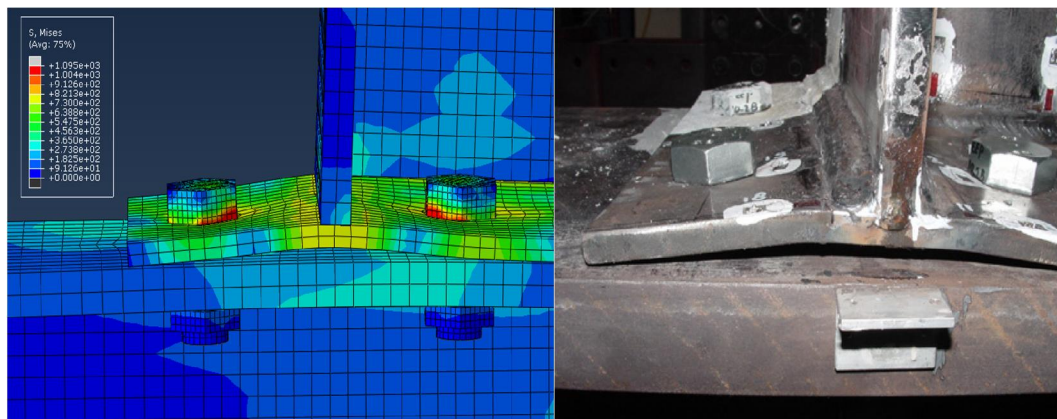
Figure 48: Moment-Rotation Curvature for Specimen P15-S690-B8.8

In this simulation by decreasing the bolt grade, it was expected to increase the connection ductility, but instead the moment resistance and connection rotation decreased. The mode of failure changed and the bolt failed before the end-plate. The

mode of failure changed to mode II. The plate in P15-S690-B8.8 had very small deformation as shown in Figure 47 and 48.

### 5.3 Comparison of Results

The first comparison is between experimental and finite element result. The behaviour of the t-stub part of the connection is shown in Figure 49. Mode of failure for t-stub according to Douty & McGuire (1965) model was mode (b), the t-stubs yield first in both experimental and finite element analysis.



(a) Finit Element Model

(b) Experimental test (Girao Coelho & Bijlaard, 2007)

Figure 49: Comparison between Finite Element Model and Experimental Test



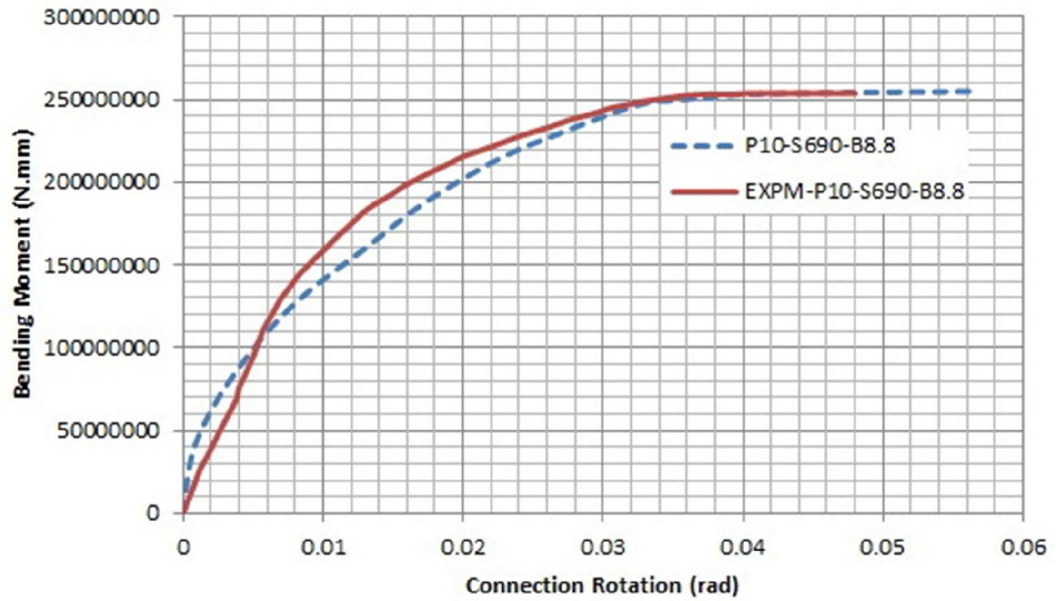


Figure 50: Comparison between Experimental and Finite Element Result of P10-S690-B8.8

According to Figure 50 the finite element result show more ductile behaviour than experimental study but the moment resistance for both of them is approximately the same.

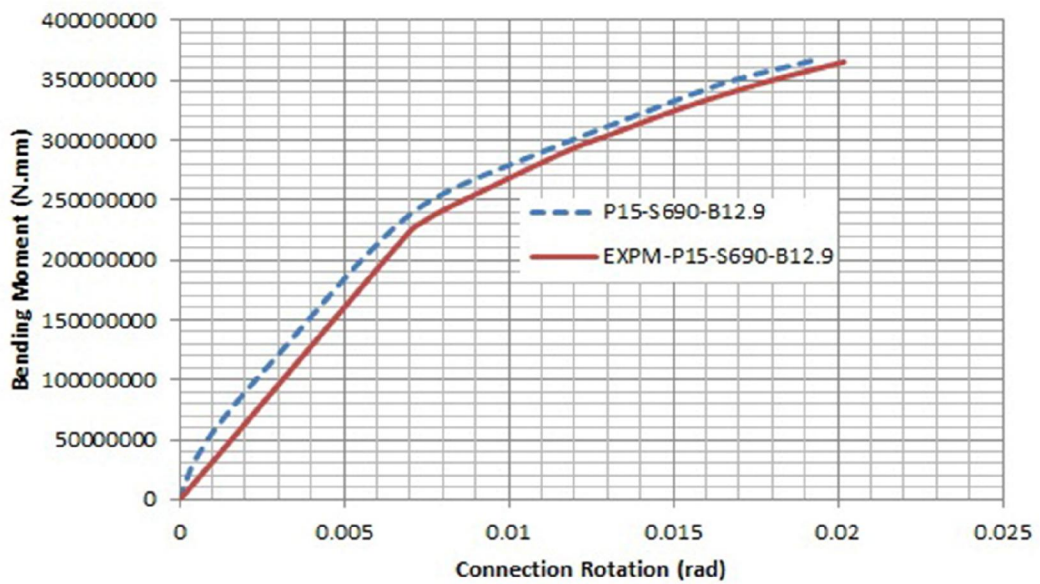


Figure 51: Comparison between Experimental and Finite Element Result of P15-S690-B12.9

According to Figure 51 the finite element analysis shown similar behaviour with experimental test for specimen P15-S690-B12.9, but the initial stiffness was higher for finite element part. The moment resistance of the connection is approximately the same but the connection rotation is lower than the experimental one.

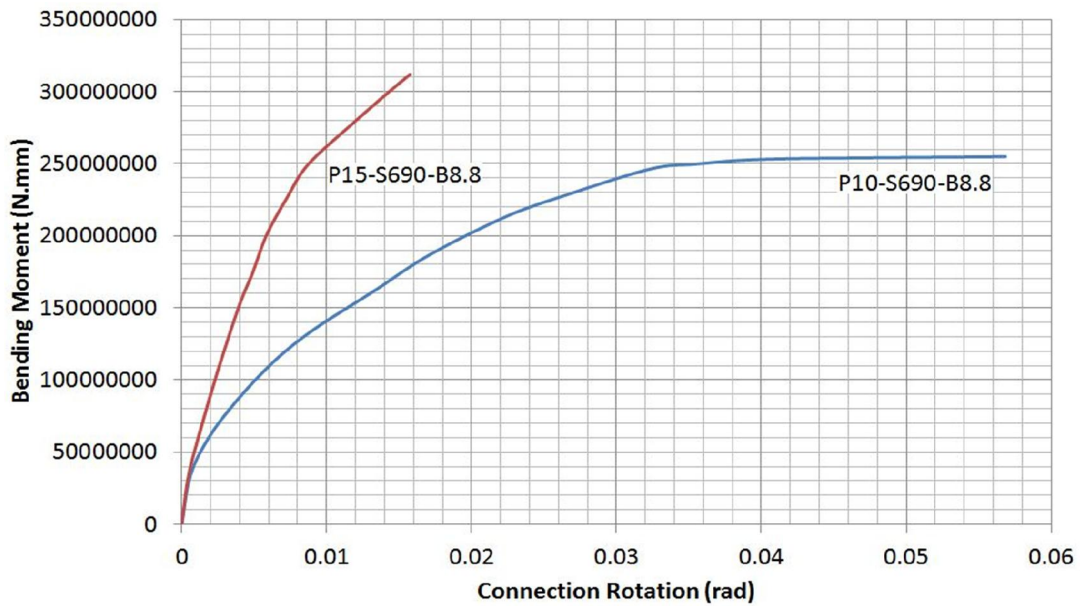


Figure 52: Comparison between 10 mm and 15 mm End-Plates with 8.8 Bolt Grades and Same End-Plate Steel Grade

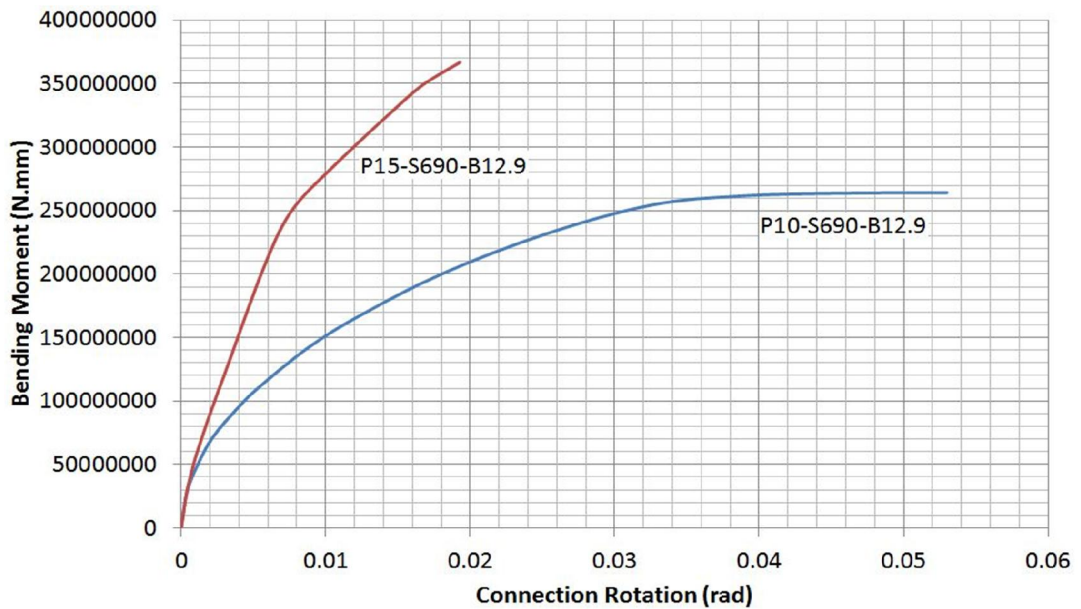


Figure 53: Comparison between 10 mm and 15 mm End-Plates with 12.9 Bolt Grades and Same End-Plate Steel Grade

As shown in Figure 52 and 53 by increasing the end-plate thickness, the ductility of the connection decreased but the moment resistance increased. The initial stiffness of the connection increased by increasing the end-plate thickness.

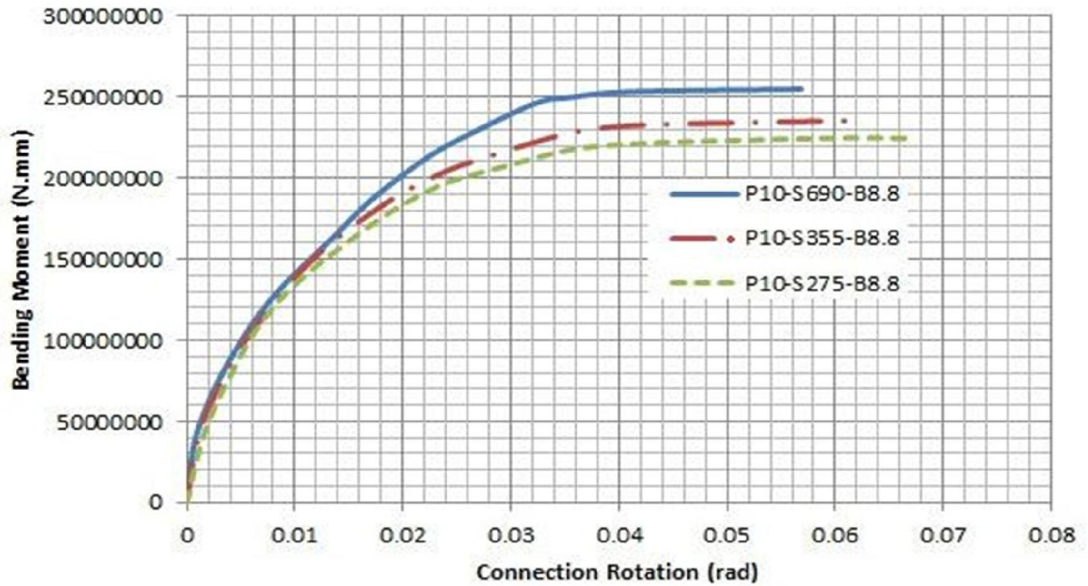


Figure 54: Comparison between End-Plates with Different Steel Grades and Same End-Plate Thickness (10 mm) and Bolt Grade 8.8

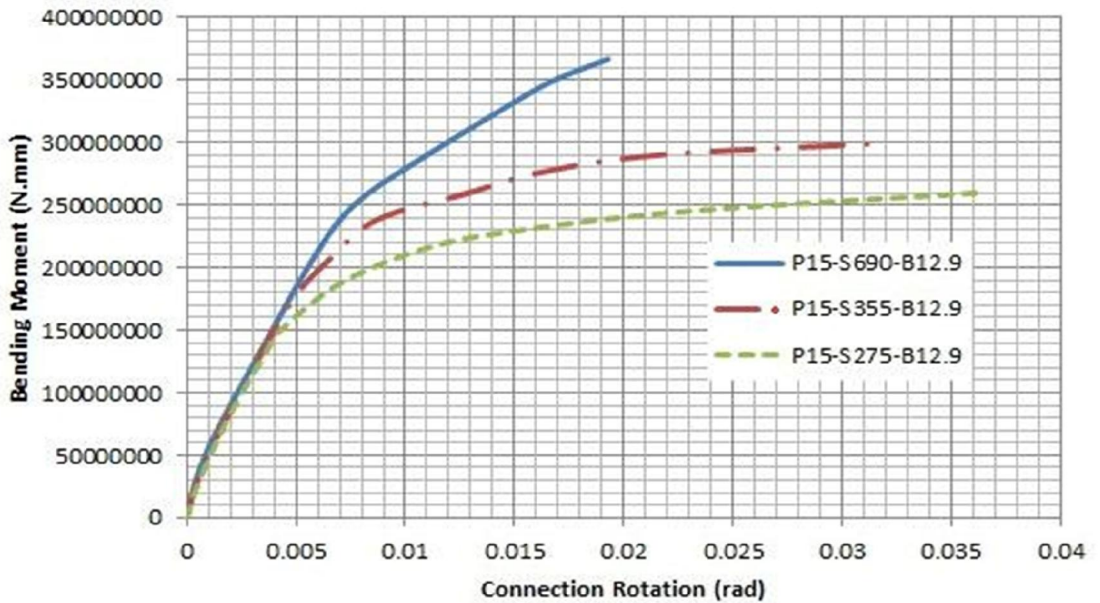


Figure 55: Comparison between End-Plates with Different Steel Grades and Same End-Plate Thickness (15 mm) and Bolt Grade 12.9



It has been demonstrated that the connection rotation increased due to decreasing the end-plate steel grade. But the moment resistance of the connection decreased. Changing the steel grade had the small effect on the initial stiffness of the connection and the initial stiffness decreased by decreasing the steel grade. This behaviour reveal for both plate thicknesses (10 and 15 mm), as shown in Figures 54 and 55.

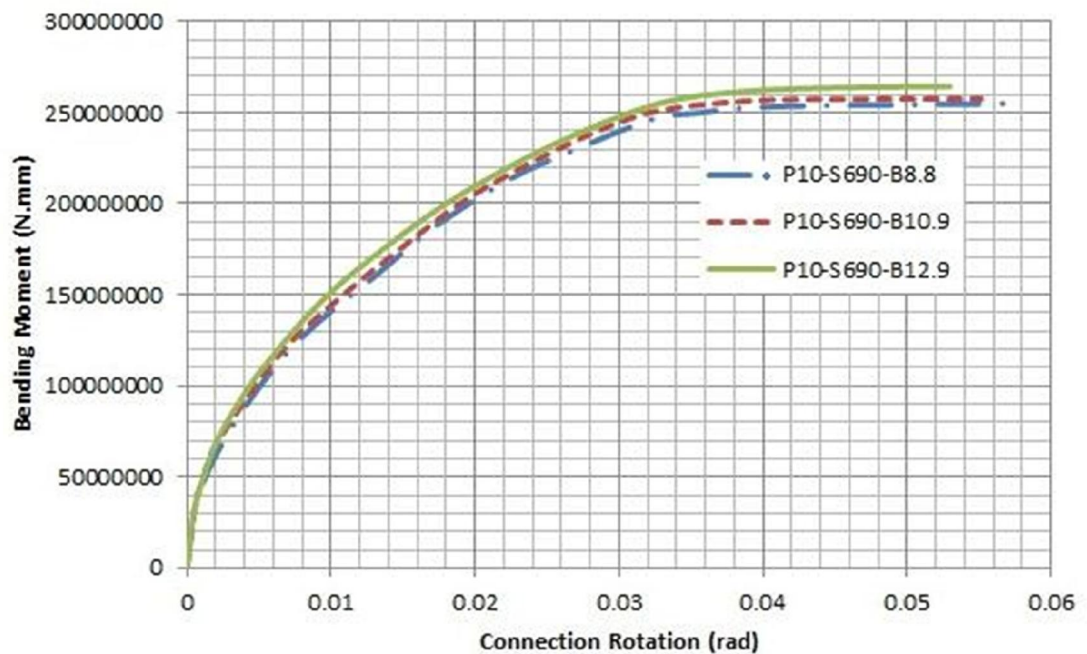


Figure 56: Comparison between End-Plates with Different Bolts Grades and Same End-Plate Thickness (10 mm) and End-Plate Grade S690

Figure 56 shows that by increasing the bolt grade little change observed in the behaviour of the connection, by increasing the bolt grade connection rotation increased and moment resistance decreased.

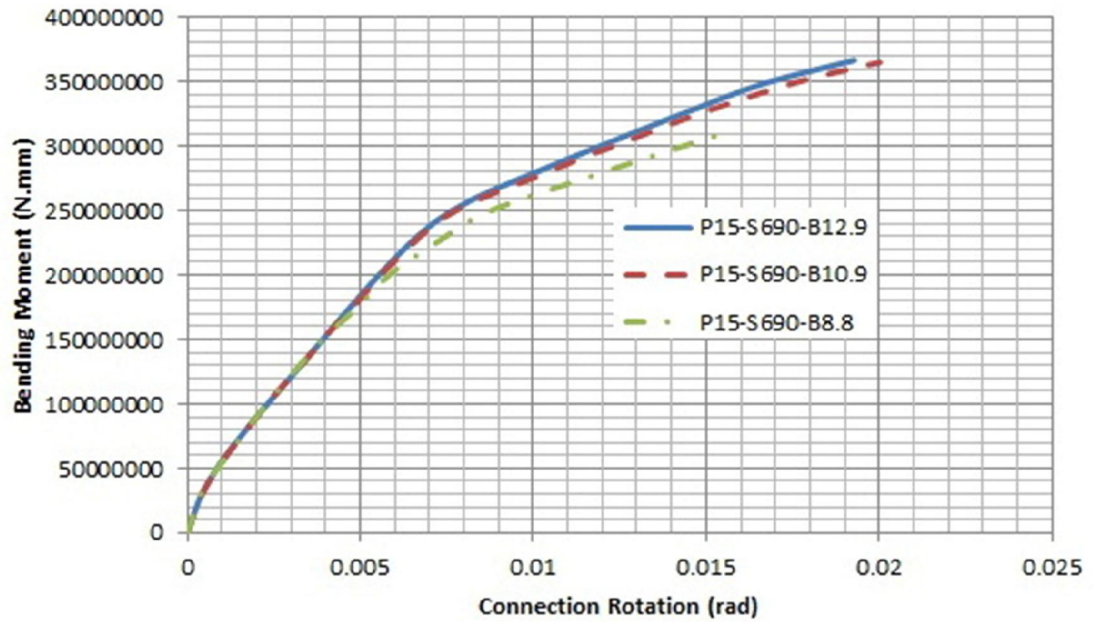


Figure 57: Comparison between End-Plates with Different Bolts Grades and Same End-Plate Thickness (15 mm) and End-Plate Grade S690

According to Figure 57, by decreasing the bolt grade from 12.9 to 10.9 the ductility was increased. This increment is caused by improvement in the plastic behaviour of the bolts. But the behaviour is changed for the connection with bolt grade 8.8. An unexpected result was observed from this simulation. The moment resistance and connection rotation was decreased. The mode of failure was changed from I to II. The bolt in the tension zone was yield first and the connection was failed. A little deformation monitored in the end-plate.

## Chapter 6

### CONCLUSIONS

#### 6.1 Summary

Using the high grade steel members has many advantages such as reduction in member's size, reduction in the weight of structure, reduction in size of the foundation and etc. (Galambos, Jerome, & Chistopher, 1997).

The high strength steel extended endplate behaviour has been investigated in this thesis under variety of the end-plate thickness and the steel grade of the end-plate and the bolts. The finite element method was used to predict the mechanical behaviour of the connection. The ABAQUS finite element software was used to model the connections and draw the moment rotation curve. In these simulations, it was tried to model all details such as contact between different components of the connection, pretension load of the bolts and nonlinear behaviour of the steel.

The finite element models are validated by comparing with the experimental results. The results show that the failure in these connections was governed by the tension zone.

#### 6.2 Conclusions

The conclusions can be observed from the simulations are:

1. By increasing the plate thickness the initial stiffness of the connection increased.

2. The moment resistance of the connection increased by increasing the plate thickness.
3. The ductility of the connection (rotation capacity) was decreased by increasing the plate thickness.
4. By decreasing the end-plate steel grade the ductility was increased but the moment resistance was decreased.
5. Bolts 12.9 have less ductility than bolts 10.9 and bolts 8.8 have more ductility than bolts 12.9 and 10.9.
6. An unexpected result was observed from the P15-S690-B8.8 simulation. The moment resistance and connection rotation was decreased. This reduction was caused by the change of the mode of failure. The bolts were yielded before the plate, for this reason the connection was not able to achieve expected ductility.
7. By using the finite element software like ABAQUS, the number of costly experimental tests can be decreased.
8. Using the finite element method is a good way to predict the behaviour of high strength steel end-plate connections.
9. The results demonstrate that high strength extended end-plate connections can be detailed and designed to be suitable for use in steel moment frames.

### **6.3 Recommendation for Further Study**

There is a need to verify the numerical part by experimental tests, and test the high strength steel flush end-plate connection and compare the behaviour of these connections.

There is a need to investigate the limit of the column flange thickness for the end-plate joints with the column flange not stiffened.

There is also a need to study the behaviour of steel members subjected to fire.

## REFERENCES

- ABAQUS inc. (2006). *ABAQUS analysis user's manual version 6.6*.
- Adey, B., Grondin, G., & Cheng, J. (1998). Extended End Plate Moment Connections Under Cyclic Loading. *J. Construct. Steel Res.*, 46, 435-436.
- Aggerskov, H. (1976). High-strength bolted connections subjected to prying. *102(ST1)*, 161-175.
- Aggerskov, H. (1977). Analysis of bolted connections subjected to prying. *103(ST11)*, 2145-2163.
- AISC. (2005). *The AISC Specification for Structural Steel Buildings*.
- Bernuzzi, C., Zandonini, R., & Zanon, P. (1991). Rotational Behaviour of End Plate Connections. *Costruzioni Metalliche*, n.2, 3-32.
- Bose, B., & Hughes, A. (1995, Nov.). Verifying the Performance of Standard Ductile Connections for Semi-Continuous Steel Frames. *Proceedings of the Institution of Civil Engineers, Structures & Buildings*, Vol. 110, pp 441-457.
- Chen, W. (2000). Practical analysis for Semi-Rigid Frame Design” Wor. *Word Scientific* .

- Chen, W., & Kishi, N. (1989). Semi-Rigid Steel Beam-to-Column connections: Database and Modeling. *Journal of Structural Engineering* *Journal of Structural Engineering*, 115, 105-119.
- Coelho, A., Bijlaard, F., & da Silva, L. (2004). Experimental assessment of the ductility of extended end plate connections. *Engineering Structures*, 26, 1185-1206.
- Díaz, C., Victoria, M., Martí, P., & Querin, O. (2011). FE model of beam-to-column extended end-plate joints. *Journal of Constructional Steel Research*, 67, 1578–1590.
- Douty, R., & McGuire, W. (1965, April). High Strength Bolted Moment Connections. *ASCE Journal of the Structural Division*, 91, 101-128.
- Eurocode 3. (1992). DD ENV 1993-1-1, Eurocode 3: Design of Steel Structures Part 1.1 General Rules and Rules for Buildings. *British Standards Institute*.
- Eurocode 3. (1997). 1.1 Joint in Building Frames (Annex J), App. *Approved Draft*, January, CEN/TC250/SC3-PT9, Comité Européen de Normalisation .
- Eurocode 3. (2005). *BS EN 1993-1-8, Eurocode 3: Design of Steel Structures Part 1-8 Design of Joints*. London: British Standards Institution.

- Galambos, T., Jerome, F., & Christopher, J. (1997). *Required properties of high-performance steels*. Maryland: National Institute of Standards and Technology.
- Girao Coelho, A. M., & Bijlaard, F. S. (2007). Experimental behaviour of high strength steel end-plate connections. *Journal of Constructional Steel Research*, 63, 1228–1240.
- Hiroshi, A. (2000). Evaluation of fractural mode of failure in steel structures following Kobe lessons. *Journal of Constructional Steel Research*, 55, 211–27.
- Kennedy, N., Vinnakota, S., & Sherbourne, A. (1981). The Split-Tee Analogy in Bolted Splices and Beam-Column Connections. *Joints in Structural Steelwork, John Wiley & sons, London-Toronto*, 2, 138-157.
- Kukreti, A., & Abolmaali, A. (1999). Moment–rotation hysteresis behavior for top and seat angle connections. *Journal of Structural Engineering ASCE*.
- Kukreti, A., Murray, T., & Abolmaali, A. (1987). End- Plate Connection Moment-Rotation Relationship. *J. Construct. Steel Research*, 8, 137-157.
- Mahin, S. (1998). Lessons from damage to steel buildings during the Northridge earthquake. *Engineering Structures*, 20, 261–70.



- Mann, A., & Morris, L. (1979). Limit design of extended end plate connections. *Journal of the Structural Division ASCE, 105(ST3)*, 511-526.
- Meng, R. (1996). Design of Moment End-Plate Connections for Seismic Loading. *Doctoral Dissertation, Virginia Polytechnic Institute and State University, Blacksburg, Virginia.*
- Nair, R., Birkemoe, P., & Munse, W. (1974, February). High Strength Bolts Subject to Tension and Prying. *ASCE Journal of the Structural Division, 100*, 351-372.
- Packer, J., & Morris, L. (1977). A Limit State Design Method for the Known Region of Bolted Beam-Column Connections. *The Structural Engineer, 55(10)*, 446-458.
- Phillips, J., & Packer, J. (1981). The effect of plate thickness on flush end-plate connections. *Proceedings of the International Conference on joints in Steelwork held at Middlesborough, Cleveland, United Kingdom Pentach Press, 6*, 77-92.
- Revised Annex J. (1994). Eurocode 3 Part 1.1 – Revised Annex J: Joints and Building Frames. *European Committee for Standardization, Document CEN/TC 250/SC3-N419E.*
- SCI. (1995). Steel Construction Institute and British Constructional Steelwork Association. *Joints in Steel Construction. Volume 1 : Moment Connections.*

- Sherbourne, A. (1961, June). Bolted Beam to Column Connexions. *The Structural Engineer*, pp 203-210.
- Sherbourne, N. A., & Mohammad, R. B. (1994). 3D Simulation of end-plate bolted connections. *Journal of Structural Engineering, ASCE*, 120(11).
- Sumner, E., Mays, T., & Murray, T. (2000, October 22-25). End-Plate Moment Connections: Test Results And Finite Element Method Validation. *Fourth International Workshop on Connections in Steel Structures, Roanoke, VA*.
- Surtees, J., & Mann, A. (1970, July). End Plate Connections in Plastically Designed Structures. *Conference on Joints in Structures*.
- Tahir, M., & Hussein, M. (2008). Experimental Tests on Extended End-Plate Connections. *Steel Structures* 8, 369-381.
- Tarpy, T., & Cardinal, J. (1981). Behavior of Semi-rigid Beam-to-Column End Plate Connections. *In Joints in Structural Steelwork, (Ed. by J.H. Howlett, W.M. Jenkins & R. Stainsby), Pentech Press*.
- van der Vegte, G. (2004, June). Numerical Simulations of Bolted Connections : the Implicit Versus the Explicit Approach. *Connections in Steel Structures V*, 90-98.

- Weynand, K., Jaspert, J., & Steenhuis, M. (1998). Economy studies of steel building frames with semi-rigid joints. *Journal of Constructional Steel Research*, 46, 1–3.
- Yee, Y., & Melchers, R. (1986, March). Moment-Rotation Curves for Bolted Connections. *ASCE Journal of the Structural Division*, 112, 615-635.
- Yorgun, C. (2002). Evaluation of Innovative Extended End-Plate Moment Connections Under Cyclic Loading. *Turkish J. Eng. Env. Sci.*, 26, 483-492.
- Zoetemeijer, P. (1974). A design method for the tension side of statically loaded, Bolted Beam-to-Column Connections. *Heron, Delft University*, 20(1), 1-59.
- Zoetemeijer, P. (1990). *Summary of the research on bolted beam-to-column*. Delft University of Technology, Faculty of Civil Engineering. Delft: Stevin Laboratory – Steel Structures.
- Zoetemeijer, P., & Munter, H. (1983). *Extended end plates with disappointing rotation capacity – Test results and analysis*. Delft University of Technology, Faculty of Civil Engineering. Delft: Stevin Laboratory Report.